California State Waters Map Series—Offshore of Carpinteria, California

By Samuel Y. Johnson, Peter Dartnell, Guy R. Cochrane, Nadine E. Golden, Eleyne L. Phillips, Andrew C. Ritchie, Rikk G. Kvitek, H. Gary Greene, Charles A. Endris, Gordon G. Seitz, Ray W. Sliter, Mercedes D. Erdey, Florence L. Wong, Carlos I. Gutierrez, Lisa M. Krigsman, Amy E. Draut, and Patrick E. Hart

(Samuel Y. Johnson and Susan A. Cochran, editors)

Pamphlet to accompany

Scientific Investigations Map 3261

2013

U.S. Department of the Interior
U.S. Geological Survey

U.S. Department of the Interior
SALLY JEWELL, Secretary

U.S. Geological Survey
Suzette M. Kimball, Acting Director

U.S. Geological Survey, Reston, Virginia: 2013

Suggested citation:
Johnson, S.Y., Dartnell, P., Cochrane, G.R., Golden, N.E., Phillips, E.L., Ritchie, A.C., Kvitek, R.G., Greene, H.G., Endris, C.A., Seitz, G.G., Sliter, R.W., Erdey, M.D., Wong, F.L., Gutierrez, C.I., Krigsman, L.M., Draut, A.E., and Hart, P.E. (S.Y. Johnson and S.A. Cochran, eds.), 2013, California State Waters Map Series—Offshore of Carpinteria, California: U.S. Geological Survey Scientific Investigations Map 3261, 42 p., 10 sheets, http://pubs.usgs.gov/sim/3261/.

Contents

Figures

Tables

Map Sheets

California State Waters Map Series—Offshore of Carpinteria, California

By Samuel Y. Johnson,[1] Peter Dartnell,[1] Guy R. Cochrane,[1] Nadine E. Golden,[1] Eleyne L. Phillips,[1] Andrew C. Ritchie,[1] Rikk G. Kvitek,[2] H. Gary Greene,[3] Charles A. Endris,[3] Gordon G. Seitz,[4] Ray W. Sliter,[1] Mercedes D. Erdey,[1] Florence L. Wong,[1] Carlos I. Gutierrez,[4] Lisa M. Krigsman,[5] Amy E. Draut,[1] and Patrick E. Hart[1]

(Samuel Y. Johnson[1] and Susan A. Cochran,[1] editors)

Preface

In 2007, the California Ocean Protection Council initiated the California Seafloor Mapping Program (CSMP), designed to create a comprehensive seafloor map of high-resolution bathymetry, marine benthic habitats, and geology within California's State Waters. The program supports a large number of coastal-zone- and ocean-management issues, including the California Marine Life Protection Act (MLPA) (California Department of Fish and Game, 2008), which requires information about the distribution of ecosystems as part of the design and proposal process for the establishment of Marine Protected Areas. A focus of CSMP is to map California's State Waters with consistent methods at a consistent scale.

The CSMP approach is to create highly detailed seafloor maps through collection, integration, interpretation, and visualization of swath sonar bathymetric data (the undersea equivalent of satellite remote-sensing data in terrestrial mapping), acoustic backscatter, seafloor video, seafloor photography, high-resolution seismic-reflection profiles, and bottom-sediment sampling data. The map products display seafloor morphology and character, identify potential marine benthic habitats, and illustrate both the surficial seafloor geology and shallow (to about 100 m) subsurface geology. It is emphasized that the more interpretive habitat and geology maps rely on the integration of multiple, new high-resolution datasets and that mapping at small scales would not be possible without such data.

This approach and CSMP planning is based in part on recommendations of the Marine Mapping Planning Workshop (Kvitek and others, 2006), attended by coastal and marine managers and scientists from around the state. That workshop established geographic priorities for a coastal mapping project and identified the need for coverage of "lands" from the shore strand line (defined as Mean Higher High Water; MHHW) out to the 3-nautical-mile (5.6-km) limit of California's State Waters. Unfortunately, surveying the zone from MHHW out to 10-m water depth is not consistently possible using ship-based surveying methods, owing to sea state (for example, waves, wind, or currents), kelp coverage, and shallow rock outcrops. Accordingly, some of the maps presented in this series commonly do not cover the zone from the shore out to 10-m depth; these "no data" zones appear pale gray on most maps.

This map is part of a series of online U.S. Geological Survey (USGS) publications, each of which includes several map sheets, some explanatory text, and a descriptive pamphlet. Each map sheet

[1] U.S. Geological Survey
[2] California State University Monterey Bay, Seafloor Mapping Lab
[3] Moss Landing Marine Laboratories, Center for Habitat Studies
[4] California Geological Survey
[5] National Oceanic and Atmospheric Administration, National Marine Fisheries Service

is published as a PDF file. Geographic information system (GIS) files that contain both ESRI[6] ArcGIS raster grids (for example, bathymetry, seafloor character) and geoTIFFs (for example, shaded relief) are also included for each publication. For those who do not own the full suite of ESRI GIS and mapping software, the data can be read using ESRI ArcReader, a free viewer that is available at http://www.esri.com/software/arcgis/arcreader/index.html (last accessed February 5, 2013).

The California Seafloor Mapping Program (CSMP) is a collaborative venture between numerous different federal and state agencies, academia, and the private sector. CSMP partners include the California Coastal Conservancy, the California Ocean Protection Council, the California Department of Fish and Game, the California Geological Survey, California State University at Monterey Bay's Seafloor Mapping Lab, Moss Landing Marine Laboratories Center for Habitat Studies, Fugro Pelagos, Pacific Gas and Electric Company (PG&E), National Oceanic and Atmospheric Administration (NOAA, including National Ocean Service – Office of Coast Surveys, National Marine Sanctuaries, and National Marine Fisheries Service), U.S. Army Corps of Engineers, the Bureau of Ocean Energy Management, the National Park Service, and the U.S. Geological Survey.

[6] Environmental Systems Research Institute, Inc.

Chapter 1.

By Samuel Y. Johnson

Regional Setting

The map area offshore of Carpinteria, California, which is referred to herein as the "Offshore of Carpinteria" map area (figs. 1–1, 1–2) lies within the central Santa Barbara Channel region of the Southern California Bight (see, for example, Lee and Normark, 2009). This geologically complex region forms a major biogeographic transition zone, separating the cold-temperate Oregonian province north of Point Conception from the warm-temperate California province to the south (Briggs, 1974).

The small city of Carpinteria (population, about 14,000) is the most significant onshore cultural center in the map area; the smaller community of Summerland (population, about 1,500) lies west of Carpinteria near the map area's western margin (fig. 1–2). Carpinteria rests on a relatively flat coastal piedmont underlain by poorly consolidated silt, sand, and gravel deposits of Holocene alluvial fans and floodplains (Minor and others, 2009), and the city is surrounded on the north, east, and west by hilly relief on the flanks of the Santa Ynez Mountains.

Southeast of Carpinteria, the coastal zone between Rincon Point and Ventura (about 15 km southeast of the map area) is characterized by a narrow (generally less than 250 m wide), low-relief coastal strip between steep coastal bluffs and the waters of the Santa Barbara Channel. This coastal strip includes a few small residential clusters and the transportation corridors for both Highway 101 and the Amtrak railway. The steep bluffs backing the coastal strip are geologically unstable; most notably, landslides in 2005 struck the small coastal community of La Conchita (fig. 1–2), engulfing houses and killing ten people.

Rincon Island lies about 900 m offshore of Punta Gorda (fig. 1–2), in the easternmost part of the map area. A man-made island, Rincon Island occupies about 2.5 acres (decreasing upward from a seafloor base of 6 acres), and it is connected to the mainland by a one-lane causeway. The island was constructed in 1958 for the specific purpose of oil and gas drilling and production.

Along the coast, Carpinteria State Beach, Carpinteria City Beach, and Rincon Beach County Park (fig. 1–2) are popular recreation destinations. Rincon Point, east of Carpinteria, is a well-known world-class surf break. El Estero, a salt marsh on the coast west of Carpinteria (fig. 1–2), is an ecologically important coastal estuary (about 230 acres), supporting many sensitive plant and animal species, as well as habitat for migrating waterfowl.

The Offshore of Carpinteria map area lies in the central part of the Santa Barbara littoral cell (fig. 1–1), which is characterized by west-to-east transport of sediment from Point Arguello on the northwest to Hueneme and Mugu Canyons on the southeast (see, for example, Griggs and others, 2005; Hapke and others, 2006). On the basis of harbor dredging records, Griggs and others (2005) estimated drift rates of about 400,000 tons/yr from Santa Barbara Harbor (about 15 km west of Carpinteria). At the east end of the littoral cell, eastward-moving sediment is trapped by Hueneme and Mugu Canyons (fig. 1–1) and then transported to the deep-water Santa Monica Basin (Normark and others, 2009).

Sediment supply to the western and central part of the littoral cell is largely from relatively small transverse coastal watersheds, which have an estimated cumulative annual sediment flux of 640,000 tons/yr (Warrick and Farnsworth, 2009). Within this map area, these coastal watersheds include (from east to west) Rincon Creek, Carpinteria Creek, Franklin Creek, Santa Monica Creek, Arroyo Paredon, and Toro Canyon Creek (fig. 1–2). The much larger Ventura and Santa Clara Rivers, the mouths of which are about 25 to 30 km southeast of Carpinteria, yield an estimated 3.4 million tons of sediment annually (Warrick and Farnsworth, 2009), the coarser sediment load generally moving southeast, down the coast, and the finer sediment load moving both upcoast and offshore (Drake, 1972; Warrick and

Farnsworth, 2009). Regionally, fluvial discharge and sediment load are highly variable, characterized by brief large events during winter storms and long periods of low or no flow and minimal sediment load between storms. In recent history, the majority of high-discharge, high-sediment-flux events have been associated with the El Niño phase of the El Niño–Southern Oscillation (ENSO) climatic pattern (Warrick and Farnsworth, 2009).

Coastal erosion problems are ongoing in the map area, and they are tied to both development and natural processes (summarized in Griggs and others, 2005; see also, Barnard and others, 2009). The shoreline is variably protected by riprap, revetments, and seawalls, perhaps most notably by nearly continuous riprap on the beaches that front El Estero (salt marsh west of Carpinteria) and also between Rincon Point and Punta Gorda (Griggs and others, 2005). In the latter area, significant amounts of sediment derived from the steep bluffs typically are not reaching the beach; instead, they are trapped and then moved away from local sites in order to keep coastal-zone transportation corridors uncovered and functional. Hapke and others (2006, their fig. 35) and Barnard and others (2009) suggested that beaches in this area have a mixed erosional-to-accretionary trend over both their long-term (between the mid-1800s and 1998) and short-term (from the mid-1970s to 1998) histories.

The Offshore of Carpinteria map area consists of a relatively flat and shallow continental shelf. The shelf dips so gently (about 0.4° to 0.5°) that water depths at the 3-nautical-mile (5.6-km) limit of California's State Waters are 40 to 45 m. This part of the Southern California Bight is relatively well protected from large Pacific swells from the north and northwest by Point Conception and from the south and southwest by offshore islands and banks (O'Reilly and Guza, 1993). Fair-weather wave base is typically shallower than 20-m water depth, but winter storms are capable of resuspending fine-grained sediments in 30 m of water (Xu and Noble, 2009, their table 7), and so shelf sediments in the map area probably are remobilized on an annual basis. As with sediment discharge from rivers, the largest wave events and the highest sediment transport rates on the shelf are typically associated with ENSO events. The shelf is underlain by variable amounts of upper Quaternary shelf, estuarine, and fluvial sediments that thicken to the south (see sheet 9 of this report; see also, Dahlen, 1992; Slater and others, 2002; Draut and others, 2009).

Seafloor habitats in the broad Santa Barbara Channel region consist of significant amounts of soft sediment and isolated areas of rocky habitat that support kelp-forest communities nearshore and rocky-reef communities in deep water. The potential marine benthic habitat types mapped in the Offshore of Carpinteria map area are directly related to its Quaternary geologic history, geomorphology, and active sedimentary processes. These potential habitats lie within the Shelf (continental shelf) megahabitat of Greene and others (2007), which is dominated by a flat seafloor and substrates that are formed from deposition of fluvial and marine sediment during sea-level rise. This fairly homogeneous seafloor provides promising habitat for groundfish, crabs, shrimp, and other marine benthic organisms. The only significant interruptions to this homogeneous habitat type are the exposures of hard, irregular, and hummocky sedimentary bedrock and coarse-grained sediment where potential habitats for rockfish (*Sebastes* spp.) and related species exist.

The Offshore of Carpinteria map area is in the Ventura Basin, in the southern part of the Western Transverse Ranges geologic province, which is north of the California Continental Borderland[7] (Fisher and others, 2009). Significant clockwise rotation—at least 90°—since the early Miocene has been proposed for the Western Transverse Ranges province (Luyendyk and others, 1980; Hornafius and others, 1986; Nicholson and others, 1994), and this region is presently undergoing north-south shortening (see, for example, Larson and Webb, 1992; Donnellan and others, 1993).

[7] The California Continental Borderland is defined as the complex continental margin that extends from Point Conception south into northern Baja California.

The active, east-west-striking, "blind" Pitas Point Fault, which cuts across the southern part of the Offshore of Carpinteria map area (sheets 8, 9, 10), is part of a north-dipping fault system that extends about 100 km below the northern part of the Santa Barbara Channel (Heck, 1998; Redin and others, 1998; Nicholson and others, 2005; Fisher and others, 2009). This fault, which crosses the shoreline offshore of Ventura (fig. 1–1), is continuous with the Ventura Fault mapped onland (see, for example, Gutierrez and others, 2008). The Ventura Avenue Anticline, which lies structurally above the Ventura–Pitas Point Fault, is presently uplifting at a rate of about 2 to 4 mm/yr (Rockwell and others, 1988); however, the rate of uplift has been as high as 12.5 mm/yr over the past 200,000 to 300,000 years (Lajoie and others, 1982, 1991). In the offshore, the Ventura Avenue Anticline is referred to as the Rincon Anticline.

The east-west-striking, steeply north-dipping Red Mountain Fault (sheets 8, 9, 10) cuts through the central part of the Offshore of Carpinteria map area, crossing the shoreline between Punta Gorda and Rincon Point (Jackson and Yeats, 1982; Tan and others, 2003a). Redin and others' (1998) cross section shows about 1,700 m of offset in the top of the Miocene Monterey Formation across the fault. Late Quaternary activity on the Red Mountain Fault is documented by about 34 m of offset on the onshore Punta Gorda marine terrace, considered to be 40,000 to 60,000 years old (Lajoie and others, 1982; Trecker and others, 1998). The east-west-striking, steeply south-dipping Rincon Creek Fault, which cuts through the northern part of the offshore map area, has been interpreted as a reverse fault in the hanging wall of the Red Mountain Fault (Jackson and Yeats, 1982; Redin and others, 1998). Jackson and Yeats (1982) suggested that the Rincon Creek Fault is also a late Quaternary structure that offsets Pleistocene strata at the surface and in the shallow subsurface, becoming a bedding-plane fault at depth.

Fault-related structures control the origins of petroleum fields in the map area (Jackson and Yeats, 1982; Redin and others, 1998). The Rincon Anticline hosts the offshore Rincon, Carpinteria, and Dos Cuadras oil fields. To the north, the Summerland oil field is in the uplifted block between the Red Mountain and Rincon Creek Faults.

An oil-well drilling accident in 1969 in the newly discovered Dos Cuadras oil field led to the Santa Barbara oil spill, a leak of between 7,000 and 70,000 barrels (Galloway, 1998). Public reaction to the spill is credited for a host of new environmental laws and regulations (Clarke and Hemphill, 2002). Although four oil wells in this map area (platforms "Hope," "Heidi," "Hazel," and "Hilda") have now been capped and their infrastructure removed (Galloway, 1998), petroleum production still continues from platforms in federal waters offshore of Carpinteria.

Publication Summary

This publication about the Offshore of Carpinteria map area includes ten map sheets that contain explanatory text, in addition to this descriptive pamphlet and a data catalog of geographic information system (GIS) files. Sheets 1, 2, and 3 combine data from four different sonar surveys to generate comprehensive high-resolution bathymetry and acoustic-backscatter coverage of the map area. These data reveal a range of physiographic features (highlighted in the perspective views on sheet 4) such as the flat, sediment-covered Santa Barbara shelf interspersed with tectonically controlled bedrock uplifts, coarse-grained deltas associated with coastal watersheds, and nearshore depositional bars. To validate the geological and biological interpretations of the sonar data shown on sheets 1, 2, and 3, the U.S. Geological Survey towed a camera sled over specific offshore locations, collecting both video and photographic imagery; this "ground-truth" surveying data is summarized on sheet 6. Sheet 5 is a "seafloor character" map, which classifies the seafloor on the basis of depth, slope, rugosity (ruggedness), and backscatter intensity and which is further informed by the ground-truth-survey imagery. Sheet 7 is a map of "potential habitats," which are delineated on the basis of substrate type, geomorphology, seafloor process, or other attributes that may provide a habitat for a specific species or

assemblage of organisms. Sheet 8 compiles representative seismic-reflection profiles from the map area, providing information on the subsurface stratigraphy and structure of the map area. Sheet 9 shows the distribution and thickness of young sediment (deposited over the last about 21,000 years, during the most recent sea-level rise) in both the map area and the larger Santa Barbara Channel region (offshore from Refugio Beach to Hueneme Canyon), interpreted on the basis of the seismic-reflection data. Sheet 10 is a geologic map that merges onshore geologic mapping (compiled from existing maps by the California Geological Survey) and new offshore geologic mapping that is based on the integration of high-resolution bathymetry and backscatter imagery (sheets 1, 2, 3), seafloor-sediment and rock samples (Reid and others, 2006), digital camera and video imagery (sheet 6), and high-resolution seismic-reflection profiles (sheet 8).

The information provided by the map sheets, pamphlet, and data catalog have a broad range of applications. High-resolution bathymetry, acoustic backscatter, ground-truth surveying imagery, and habitat mapping all contribute to habitat characterization and ecosystem-based management by providing essential data for delineation of marine protected areas and ecosystem restoration. Many of the maps provide high-resolution baselines that will be critical for monitoring environmental change associated with climate change, coastal development, or other forcings. High-resolution bathymetry is a critical component for modeling coastal flooding caused by storms and tsunamis, as well as inundation

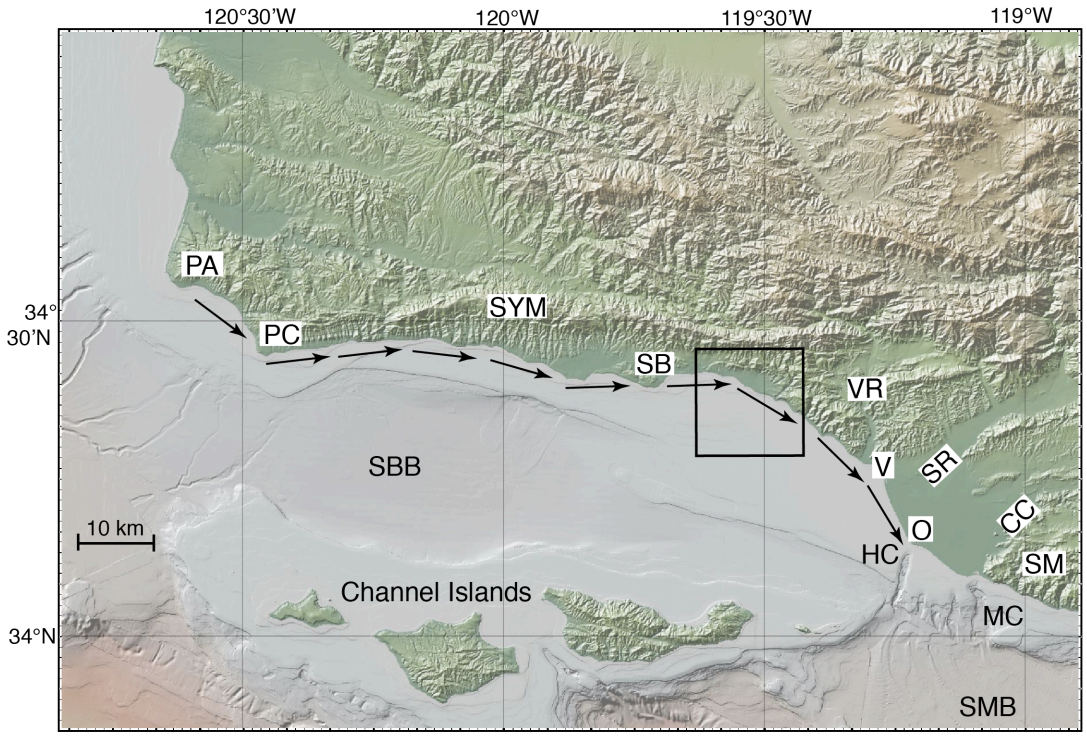

Figure 1–1. Physiography of Santa Barbara Channel region. Box shows Offshore of Carpinteria map area. Arrows show direction of sediment transport in Santa Barbara littoral cell, which extends from Point Arguello (PA) to Hueneme Canyon (HC) and Mugu Canyon (MC). Other abbreviations: CC, Calleguas Creek; O, Oxnard; PC, Point Conception; SB, Santa Barbara; SBB, Santa Barbara Basin; SM, Santa Monica Mountains; SMB, Santa Monica Basin; SR, Santa Clara River; SYM, Santa Ynez Mountains; V, Ventura; VR, Ventura River.

associated with longer term sea-level rise. Seismic-reflection and bathymetric data help characterize earthquake and tsunami sources, critical for natural-hazard assessments of coastal zones. Information on sediment distribution and thickness is essential to the understanding of local and regional sediment transport, as well as the development of regional sediment-management plans. New high-resolution bathymetric data can be used to update nautical charts, thereby enhancing safety for navigation and commerce. In addition, the siting of any new offshore infrastructure (for example, pipelines, cables, or renewable-energy facilities) also will depend on high-resolution mapping. Finally, this mapping will both stimulate and enable new scientific research and also raise public awareness of, and education about, coastal environments and issues.

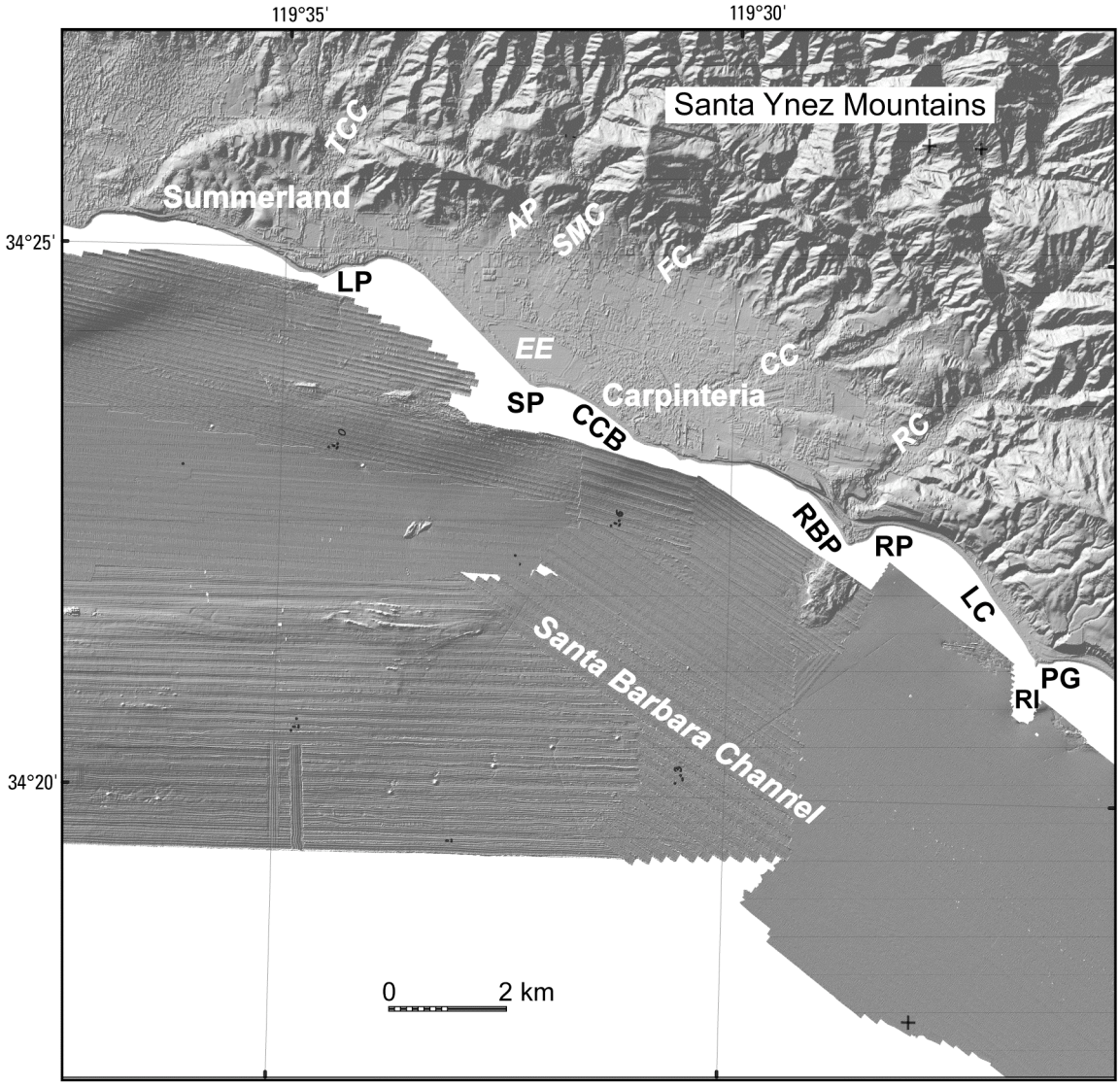

Figure 1–2. Coastal geography of Offshore of Carpinteria map area. Abbreviations: AP, Arroyo Paredon; CC, Carpinteria Creek; CCB, Carpinteria City Beach and Carpinteria State Beach; EE, El Estero (salt marsh west of Carpinteria); FC, Franklin Creek; LC, La Conchita; LP, Loon Point; PG, Punta Gorda; RBP, Rincon Beach County Park; RC, Rincon Creek; RI, Rincon Island; RP, Rincon Point; SMC, Santa Monica Creek; SP, Sand Point; TCC, Toro Canyon Creek.

Chapter 2. Bathymetry and Backscatter-Intensity Maps of the Offshore of Carpinteria Map Area (Sheets 1, 2, and 3)

By Peter Dartnell and Rikk G. Kvitek

The colored shaded-relief bathymetry (sheet 1), the shaded-relief bathymetry (sheet 2), and the acoustic-backscatter (sheet 3) maps of the Offshore of Carpinteria map area in southern California were generated from bathymetry and backscatter data collected by California State University, Monterey Bay (CSUMB), by the U.S. Geological Survey (USGS), and by Fugro Pelagos for the U.S. Army Corps of Engineers (USACE) Joint Lidar Bathymetry Technical Center of Expertise (fig. 1 on sheets 1, 2, 3). The southeastern nearshore and shelf areas, as well as the western midshelf area, were mapped by CSUMB in the summer of 2007, using a 244-kHz Reson 8101 multibeam echosounder. The western nearshore area, as well as the western outer shelf area, were mapped by the USGS in 2005 and 2006, using 117-kHz and 234.5-kHz SEA (AP) Ltd. SWATHplus-M phase-differencing sidescan sonars. The nearshore bathymetry and coastal topography were mapped for USACE by Fugro Pelagos in 2009, using the SHOALS-1000T bathymetric-lidar and Leica ALS60 topographic-lidar systems. All these mapping missions combined to collect both bathymetry (sheets 1, 2), from the 0-m isobath to beyond the 3-nautical-mile limit of California's State Waters, and acoustic-backscatter data (sheet 3), from about the 10-m isobath to beyond the 3-nautical-mile limit.

During the CSUMB mapping mission, an Applanix position and motion compensation system (POS/MV) was used to accurately position the vessel during data collection, and it also accounted for vessel motion such as heave, pitch, and roll (position accuracy, ±2 m; pitch, roll, and heading accuracy, ±0.02°; heave accuracy, ±5%, or 5 cm). NavCom 2050 GPS receiver (CNAV) data were used to account for tidal-cycle fluctuations, and sound-velocity profiles were collected with an Applied Microsystems (AM) SVPlus sound velocimeter. Soundings were corrected for vessel motion using the Applanix POS/MV data, for variations in water-column sound velocity using the AM SVPlus data, and for variations in water height (tides) using vertical-position data from the CNAV receiver. Final XYZ soundings and bathymetric-surface models were referenced to the World Geodetic System of 1984 (WGS 1984) relative to the North American Vertical Datum of 1988 (NAVD 1988) (Kvitek, 2007). Backscatter data then were postprocessed using CARIS7.0/Geocoder software. Geobars were created for each survey line using the beam-averaging engine. Intensities were radiometrically corrected (including despeckling and angle-varying gain adjustments), and the position of each acoustic sample was geometrically corrected for slant range on a line-by-line basis. The contrast and brightness of some geobars were adjusted to better match the surrounding geobars. Individual geobars were mosaicked together at 2-m resolution using the auto-seam method. The mosaics were then exported from CARIS as georeferenced TIFF images, imported into a geographic information system (GIS), and converted to GRIDs.

During the USGS mapping missions, differential GPS (DGPS) data were combined with measurements of vessel motion (heave, pitch, and roll) in a CodaOctopus F180 attitude-and-position system to produce a high-precision vessel-attitude packet. This packet was transmitted to the acquisition software in real time and combined with instantaneous sound-velocity measurements at the transducer head before each ping. The returned samples were projected to the seafloor using a ray-tracing algorithm that works with previously measured sound-velocity profiles. Statistical filters were applied to the raw samples that discriminate the seafloor returns (soundings) from unintended targets in the water column. The original soundings were referenced to the WGS 1984 relative to the MLLW (Mean Lower Low Water) tidal datum, but, through postprocessing using National Oceanic and Atmospheric Administration's (NOAA's) VDatum tool, the soundings were transformed to NAVD 1988. Finally, the

soundings were converted into 2-m-resolution bathymetric-surface-model grids. The backscatter data were postprocessed using USGS software (D.P. Finlayson, written commun., 2011) that normalizes for time-varying signal loss and beam-directivity differences. Thus, the raw 16-bit backscatter data were gain-normalized to enhance the backscatter of the SWATHplus system. The resulting normalized-amplitude values were rescaled to 16-bit and gridded into GeoJPEGs using GRID Processor Software, then imported into a GIS and converted to GRIDs.

During the Fugro Pelagos mapping mission that was completed as part of the National Coastal Mapping Program of USACE, the Leica ALS60 topographic-lidar and the SHOALS-1000T bathymetric-lidar systems were mounted on an aircraft that flew survey lines at an altitude of 300 to 400 m (bathymetry) and 300 to 1,200 m (topography), at speeds of between 135 and 185 knots. The ALS60 system collected data at a maximum pulse rate of 200 kHz, and the SHOALS system collected data at 1 kHz. Information on aircraft position, velocity, and acceleration were collected using the Novatel and POS A/V 410 systems (SHOALS) and the onboard GPS/IMU system (ALS60). Aircraft-position data were processed using POSPac software, and the results were combined with the lidar data to produce 3-D positions for each lidar shot. Various commercial and proprietary software packages were used to clean the data, to convert all valid data from ellipsoid to orthometric heights, and to export the data as a series of topography and bathymetry ASCII files. Final grids were provided in geographic coordinates referenced to the NAVD 1988.

Once all the bathymetric-surface models were transformed to a common projection and datum, the files were merged into one overall 2-m-resolution bathymetric-surface model and clipped to the boundary of the map area. Difference calculations of the overlapping bathymetry grids showed that there is good agreement between surveys, even though the surveys were conducted at different times using different mapping equipment. For example, a mean difference of 0.08 m (0.20 standard deviation) exists between the 2007 CSUMB multibeam-echosounder data and the overlapping 2005 USGS SWATHplus data in the central part of the map area. A mean difference of 0.16 m (0.26 standard deviation) also is present between the 2006 USGS SWATHplus data and the overlapping 2009 USACE bathymetric-lidar data, even though the overlap is in the energetic nearshore region that is highly susceptible to natural change.

An illumination having an azimuth of 300° and from 45° above the horizon was then applied to the bathymetric surface to create the shaded-relief imagery (sheets 1, 2). In addition, a modified "rainbow" color ramp was applied to the bathymetry data for sheet 1, using reds and oranges to represent shallower depths, and light greens to represent greater depths (note that the Offshore of Carpinteria map area requires only the shallower part of the full-rainbow color ramp used on some of the other maps in the California State Waters Map Series; see, for example, Kvitek and others, 2012). This colored bathymetry surface was draped over the shaded-relief imagery at 60-percent transparency to create a colored shaded-relief map (sheet 1).

Bathymetric contours (sheets 1, 2, 3, 7, 10) were generated from a modified bathymetric surface of California's State Waters within the Santa Barbara Channel. This surface was generated by merging all of California Seafloor Mapping Program's bathymetry data for the region into one surface model. After merging, the surface model was resampled to 10-m resolution, and then a smooth arithmetic mean convolution function that assigns a weight of one-ninth to each cell in a 3-pixel by 3-pixel matrix was applied iteratively to the surface ten times. Following smoothing, contour lines were generated at 10-m intervals, from -10 m to -100 m, and at 50-m intervals, from -100 m to -400 m, then the contours were clipped to the boundary of the map area.

Similarly, once all the acoustic-backscatter images were transformed to a common projection, the grids were combined in a GIS to create an acoustic-backscatter map (sheet 3), on which brighter tones indicate higher backscatter intensity, and darker tones indicate lower backscatter intensity. The intensity represents a complex interaction between the acoustic pulse and the seafloor, as well as

characteristics within the shallow subsurface, providing a general indication of seafloor texture and sediment type. Backscatter intensity depends on the acoustic source level; the frequency used to image the seafloor; the grazing angle; the composition and character of the seafloor, including grain size, water content, bulk density, and seafloor roughness; and some biological cover. Harder and rougher bottom types such as rocky outcrops or coarse sediment typically return stronger intensities (high backscatter, lighter tones), whereas softer bottom types such as fine sediment return weaker intensities (low backscatter, darker tones). The differences in backscatter intensity that are apparent in some areas on sheet 3 are due to the different frequencies of mapping systems, as well as different processing techniques.

The onshore-area image was generated by applying an illumination having an azimuth of 300° and from 45° above the horizon to the coastal airborne topographic-lidar data, as well as to publicly available, 3-m-resolution, interferometric synthetic aperture radar (ifSAR) data, available from NOAA Coastal Service Center's Digital Coast (National Oceanic and Atmospheric Administration, 2011).

Chapter 3. Data Integration and Visualization for the Offshore of Carpinteria Map Area (Sheet 4)

By Peter Dartnell

Mapping California's State Waters has produced a vast amount of acoustic and visual data, including bathymetry, acoustic backscatter, seismic-reflection profiles, and seafloor video and photography. These data are used by researchers to develop maps, reports, and other tools to assist in the coastal and marine spatial-planning capability of coastal-zone managers and other stakeholders. For example, seafloor-character (sheet 5), habitat (sheet 7), and geologic (sheet 10) maps of the Offshore of Carpinteria map area are used to assist in the designation of Marine Protected Areas, as well as in their monitoring. These maps and reports also help to analyze environmental change owing to sea-level rise and coastal development, to model and predict sediment and contaminant budgets and transport, to site offshore infrastructure, and to assess tsunami and earthquake hazards. To facilitate this increased understanding and to assist product development, it is helpful to integrate the different datasets and then view the results in three-dimensional representations such as those displayed on the data integration and visualization sheet for the Offshore of Carpinteria map area (sheet 4).

The maps and three-dimensional views on sheet 4 were created using a series of geographic information systems (GIS) and visualization techniques. Using GIS, the bathymetric and topographic data (sheet 1) were converted to ASCIIRASTER format files, and the acoustic-backscatter data (sheet 3) were converted to geoTIFF images. The bathymetric and topographic data were imported in the Fledermaus® software (QPS). The bathymetry was color-coded to closely match the colored shaded-relief bathymetry on sheet 1 in which reds and oranges represent shallower depths and light greens represent deeper depths. Topographic data were shown in gray shades. The acoustic-backscatter geoTIFF images were also draped over the bathymetry data. The colored bathymetry, topography, and draped backscatter were then tilted and panned to create the perspective views such as those shown in figures 1, 2, 3, 5, and 6 on sheet 4. These figures highlight the relatively small scale (2 to 10 m) of the seafloor features along the broad continental shelf in the eastern Santa Barbara Channel.

Video-mosaic images created from digital seafloor video (for example, fig. 4 on sheet 4) display the geologic complexity (rock, sand, and mud; see sheet 10) and biologic complexity of the seafloor. Whereas photographs capture high-quality snapshots of smaller areas of the seafloor (see sheet 6), video mosaics capture larger areas and can show transition zones between seafloor environments. Digital seafloor video is collected from a camera sled towed approximately 1 to 2 meters over the seafloor, at speeds less than 1 nautical mile/hour. Using standard video-editing software, as well as software developed at the Center for Coastal and Ocean Mapping, University of New Hampshire, the digital video is converted to AVI format, cut into 2-minute sections, and desampled to every second or third frame. The frames are merged together using pattern-recognition algorithms from one frame to the next and converted to a TIFF image. The images are then rectified to the bathymetry data using ship navigation recorded with the video and layback estimates.

Block diagrams that combine the bathymetry with seismic-reflection profile data help integrate surface and subsurface observations, especially stratigraphic and structural relations (for example, fig. 6 on sheet 4). These block diagrams were created by converting digital seismic-reflection profile data (Sliter and others, 2008) into TIFF images, while taking note of the starting and ending coordinates and maximum and minimum depths. The images were then imported into the Fledermaus® software as vertical images and merged with the bathymetry imagery.

Chapter 4. Seafloor-Character Map of the Offshore of Carpinteria Map Area (Sheet 5)

By Eleyne L. Phillips, Mercedes D. Erdey, and Guy R. Cochrane

The California State Marine Life Protection Act (MLPA) calls for protecting representative types of habitat in different depth zones and environmental conditions. A science team, assembled under the auspices of the California Department of Fish and Game (CDFG), has identified seven substrate-defined seafloor habitats in California's State Waters that can be classified using sonar data and seafloor video and photography. These habitats include rocky banks, intertidal zones, sandy or soft ocean bottoms, underwater pinnacles, kelp forests, submarine canyons, and seagrass beds. The following five depth zones, which determine changes in species composition, have been identified: Depth Zone 1, intertidal; Depth Zone 2, intertidal to 30 m; Depth Zone 3, 30 to 100 m; Depth Zone 4, 100 to 200 m; and Depth Zone 5, deeper than 200 m (California Department of Fish and Game, 2008). The CDFG habitats, with the exception of depth zones, can be considered a subset of a broader classification scheme of Greene and others (1999) that has been used by the U.S. Geological Survey (USGS) (Cochrane and others, 2003, 2005). These seafloor-character maps are generalized polygon shapefiles that have attributes derived from Greene and others (2007).

A 2007 Coastal Map Development Workshop, hosted by the USGS in Menlo Park, California, identified the need for more detailed (relative to Greene and others' [1999] attributes) raster products that preserve some of the transitional character of the seafloor when substrates are mixed and (or) they change gradationally. The seafloor-character map, which delineates a subset of the CDFG habitats, is a GIS-derived raster product that can be produced in a consistent manner from data of variable quality covering large geographic regions.

The following five substrate classes are identified in the Offshore of Carpinteria map area:

- Class I: Fine- to medium-grained smooth sediment
- Class II: Mixed smooth sediment and rock
- Class III: Rock and boulder, rugose
- Class IV: Anthropogenic material (rugged)
- Class V: Anthropogenic material (smooth, hard)

The seafloor-character map of the Offshore of Carpinteria map area (sheet 5) was produced using video-supervised maximum-likelihood classification of the bathymetry and intensity of return from sonar systems, following the method described by Cochrane (2008). The two variants used in this classification were backscatter intensity and derivative rugosity, which is a standard calculation performed with the National Oceanic and Atmospheric Administration (NOAA) benthic-terrain modeler (available at http://www.csc.noaa.gov/digitalcoast/tools/btm/index.html; last accessed April 5, 2011), using a 3-pixel by 3-pixel array of bathymetry.

Classes I, II, and III were delineated using multivariate analysis. Class IV (rugged anthropogenic material) and Class V (smooth, hard anthropogenic material) values were determined on the basis of their visual characteristics and the known location of man-made features. The resulting map (gridded at 2 m) was cleaned by hand to remove data-collection artifacts (for example, the trackline nadir).

On the seafloor-character map (sheet 5), the five substrate classes have been colored to indicate the California MLPA depth zones and the Coastal and Marine Ecological Classification Standard (CMECS) slope zones (Madden and others, 2008) in which they belong. The California MLPA depth zones are Depth Zone 1 (intertidal), Depth Zone 2 (intertidal to 30 m), Depth Zone 3 (30 to 100 m),

Depth Zone 4 (100 to 200 m), and Depth Zone 5 (greater than 200 m); in the Offshore of Carpinteria map area, only Depth Zones 2 and 3 are present. The slope classes that represent the CMECS slope zones are Slope Class 1 = flat (0° to 5°), Slope Class 2 = sloping (5° to 30°), Slope Class 3 = steeply sloping (30° to 60°), Slope Class 4 = vertical (60° to 90°), and Slope Class 5 = overhang (greater than 90°); in the Offshore of Carpinteria map area, only Slope Class 1 is present. The final classified seafloor-character raster map image is draped over the shaded-relief bathymetry for the area (sheets 1 and 2) to produce the image shown on the seafloor-character map on sheet 5.

The seafloor-character classification is also summarized on sheet 5 in table 1. Fine- to medium-grained smooth sediment (sand and mud) makes up 98.0 percent of the map area (139.1 km^2): 47.0 km^2 is in Depth Zone 2, and 92.1 km^2 is in Depth Zone 3. Mixed smooth sediment (sand and gravel) and rock (sediment typically forming a veneer over bedrock, or rock outcrops having little to no relief) make up 1.6 percent of the area mapped (2.3 km^2): 1.2 km^2 is in Depth Zone 2, and 1.1 km^2 is in Depth Zone 3. Rock and boulder, rugose (rock and boulder outcrops having high surficial complexity) make up 0.3 percent of the map area (0.4 km^2): 0.4 km^2 is in Depth Zone 2, and less than 0.1 km^2 is in Depth Zone 3. Rugged anthropogenic material (oil-platform structural support) makes up 0.1 percent of the map area (0.1 km^2): less than 0.1 km^2 is in Depth Zone 2, and 0.1 km^2 is in Depth Zone 3. Smooth, hard anthropogenic material (shell-hash mound adjacent to platform) makes up less than 0.1 percent of the map area (<0.1 km^2): less than 0.1 km^2 is in Depth Zone 2, and less than 0.1 km^2 is in Depth Zone 3.

A small number of video observations were used to supervise the numerical classification of the seafloor. All video observations (see sheet 6) are used for accuracy assessment of the seafloor-character map after classification. To compare observations to classified pixels, each observation point is assigned a class (I, II, or III), according to either the visually derived, major or minor geologic component (for example, sand or rock) and the abiotic complexity (vertical variability) of the substrate (table 4–1). Class IV and Class V values are determined from the visual characteristics and known location of man-made features. Next, circular buffer areas are created around individual observation points using a 10-m radius to account for layback and positional inaccuracies inherent to the towed-camera system. The radius length is an average of the distances between the positions of sharp interfaces seen on both the video (the position of the ship at the time of observation) and sonar data, plus the distance covered during a 10-second observation period at an average speed of 1 nautical mile/hour. Each buffer, which covers more than 300 m^2, contains approximately 77 pixels. The classified (I, II, III) buffer is used as a mask to extract pixels from the seafloor-character map. These pixels are then compared to the class of the buffer. For example, if the shipboard-video observation is Class II (mixed smooth sediment and rock), but 12 of the 77 pixels within the buffer area are characterized as Class I (fine- to medium-grained smooth sediment), and 15 (of the 77) are characterized as Class III (rock and boulder, rugose), then the comparison would be “Class I, 12; Class II, 50; Class III, 15” (fig. 4–1). If the video observation of substrate is Class II, then the classification is accurate because the majority of seafloor pixels in the buffer are Class II. The accuracy values in table 4–2 represent the final of several classification iterations aimed at achieving the best accuracy, given the variable quality of sonar data (see discussion in Cochrane, 2008) and the limited ground-truth information available when compared to the continuous coverage provided by swath sonar. Presence/absence values in table 4–2 reflect the percentages of observations where the sediment classification of at least one pixel within the buffer zone agreed with the observed sediment type at a certain location.

The seafloor in the Offshore of Carpinteria map area is mainly flat with local, small sedimentary-bedrock exposures (Class III). The seabed is predominantly covered by Class I sediment composed of sand and mud. An area of small rock exposures (Class III) is present further offshore of Carpinteria, near the 3-nautical-mile limit of California’s State Waters; exposed rock is covered intermittently by varying thicknesses of fine- (Class I) to coarse-grained (Class II) sediment (coarse sand and gravel). Several

anthropogenic features associated with oil production are present, including platforms and pipelines, jetties and groins, and shell mounds beneath platforms.

The classification accuracy of Class I (87 percent accurate; table 4–2) is determined by comparing the shipboard video observations and the classified map. The weaker agreement in Classes II and III (42 percent and 19 percent, respectively) likely is due to the distribution of localized small rock outcrops and the relatively narrow, intermittent nature of transition zones from sediment to rock, as well as the size of the buffer. The bedrock outcrops in this area are composed of sedimentary rocks exhibiting differential erosion (Cochrane and Lafferty, 2002). Erosion of softer layers produces Class I and II sediments, resulting in patchy rugose rock and boulder habitat on the seafloor. A single buffered observation locality of 78 pixels, therefore, is likely to be interspersed with other classes of pixels in addition to Class III. Percentages for presence/absence within a buffer also were calculated as a better measure of the accuracy of classification for patchy rock habitat. The presence/absence accuracy was found to be significant for all classes (100 percent for Class I, 93 percent for Class II, and 61 percent for Class III). No video observations were retrieved over the anthropogenic features associated with oil production (Class IV substrate, rugged anthropogenic feature; Class V substrate, smooth, hard anthropogenic feature).

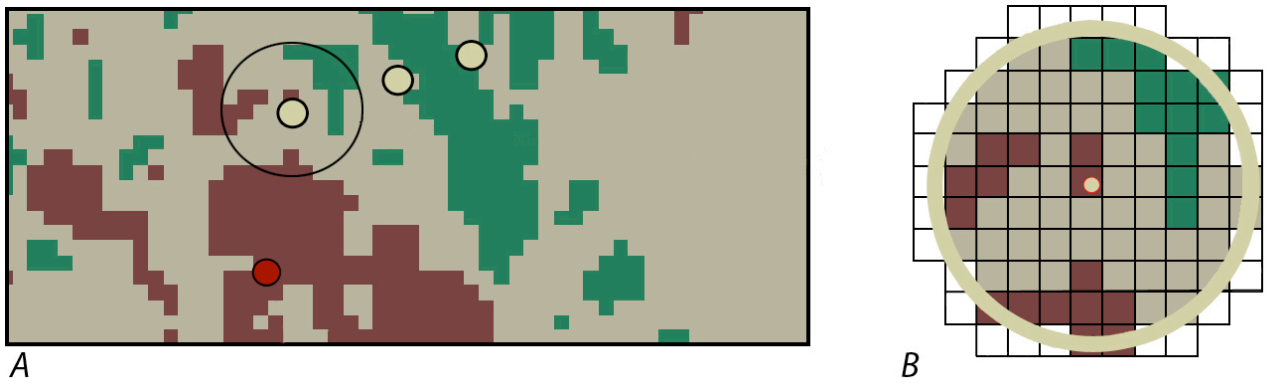

Figure 4–1. Detailed view of ground-truth data, showing accuracy-assessment methodology. *A*, Dots illustrate ground-truth observation points, each of which represents 10-second window of substrate observation plotted over seafloor-character grid; circle around dot illustrates area of buffer depicted in *B*. *B*, Pixels of seafloor-character data within 10-m-radius buffer centered on one individual ground-truth video observation.

Table 4–1. Conversion table showing how video observations of primary substrate (more than 50 percent seafloor coverage), secondary substrate (more than 20 percent seafloor coverage), and abiotic seafloor complexity (in first three columns) are grouped into seafloor-character-map Classes I, II, and III for use in supervised classification and accuracy assessment.

[In areas of low visibility where primary and secondary substrate could not be identified with confidence, recorded observations of substrate (in fourth column) were used to assess accuracy]

Primary-substrate component	Secondary-substrate component	Abiotic seafloor complexity	Low-visibility observations
Class I			
mud	mud	low	
mud	shell hash	low	
mud	shell hash	moderate	
mud	sand	low	
shell hash	mud	low	
shell hash	mud	moderate	
sand	mud	low	
sand	mud	moderate	
sand	sand	low	
			sedimented
			high mud component
			mud component
			nepheloid
Class II			
boulders	cobbles	low	
boulders	sand	low	
cobbles	boulders	low	
cobbles	cobbles	low	
cobbles	cobbles	moderate	
cobbles	mud	moderate	
cobbles	sand	low	
cobbles	sand	moderate	
mud	rock	low	
rock	cobbles	low	
rock	mud	low	
rock	sand	low	
sand	boulders	low	
sand	boulders	moderate	
sand	cobbles	low	
sand	cobbles	moderate	
sand	shell hash	low	
sand	rock	low	
sand	rock	moderate	

Table 4–1. Conversion table showing how video observations of primary substrate, secondary substrate, and abiotic seafloor complexity are grouped into seafloor-character-map Classes I, II, and III for use in supervised classification and accuracy assessment.—*Continued*

Primary-substrate component	Secondary-substrate component	Abiotic seafloor complexity	Low-visibility observations
Class III			
boulders	boulders	moderate	
boulders	boulders	high	
boulders	cobbles	moderate	
boulders	rock	moderate	
boulders	rock	high	
boulders	sand	moderate	
boulders	sand	high	
boulders	boulders	moderate	
cobbles	boulders	moderate	
mud	boulders	moderate	
mud	rock	moderate	
rock	boulders	moderate	
rock	boulders	high	
rock	cobbles	moderate	
rock	mud	moderate	
rock	rock	moderate	
rock	rock	high	
rock	sand	moderate	

Table 4–2. Accuracy assessment statistics for seafloor-character-map classifications.

[Accuracy assessments are based on video observations and sediment samples (N/A, no accuracy assessment was conducted)]

Class	Number of observations	% majority	% presence/absence
I—Fine- to medium-grained smooth sediment	463	86.9	99.8
II—Mixed smooth sediment and rock	106	42.4	93.4
III—Rock and boulder, rugose	218	18.5	61.0
IV—Rugged anthropogenic feature	0	N/A	N/A
V—Smooth, hard anthropogenic feature	0	N/A	N/A

Chapter 5. Ground-Truth Studies for the Offshore of Carpinteria Map Area (Sheet 6)

By Nadine E. Golden and Guy R. Cochrane

To validate the interpretations of sonar data in order to turn it into geologically and biologically useful information, the U.S. Geological Survey (USGS) towed a camera sled (fig. 5–1) over specific locations throughout the Offshore of Carpinteria map area to collect video and photographic data that would "ground truth" the seafloor. This ground-truth surveying occurred on three separate cruises in 2005, 2006, and 2008. The camera sled was towed 1 to 2 m over the seafloor at speeds of between 1 and 2 nautical miles/hour. Ground-truth surveys in this map area include approximately 31.72 trackline kilometers of video and 31 still photographs, in addition to 1,038 recorded seafloor observations of abiotic and biotic attributes. A visual estimate of slope also was recorded.

During the 2005 and 2006 cruises, a smaller USGS camera sled was used that housed two video cameras: one was forward looking, and the other was downward looking. During the 2008 cruise, a larger camera sled was used that housed two video cameras (one forward looking and one downward looking), a high-definition video camera, and an 8-megapixel digital still camera. During this cruise, in addition to recording the seafloor characteristics, a digital still photograph was captured once every 30 seconds.

The camera-sled tracklines (shown by colored dots on the map on sheet 6) are sited in order to visually inspect areas representative of the full range of bottom hardness and rugosity in the map area. The video is fed in real time to the research vessel, where USGS and National Oceanic and Atmospheric Administration (NOAA) scientists record both the geologic and biologic character of the seafloor. While the camera is deployed, several different observations are recorded for a 10-second period once every minute, using the protocol of Anderson and others (2007). Observations of primary substrate, secondary

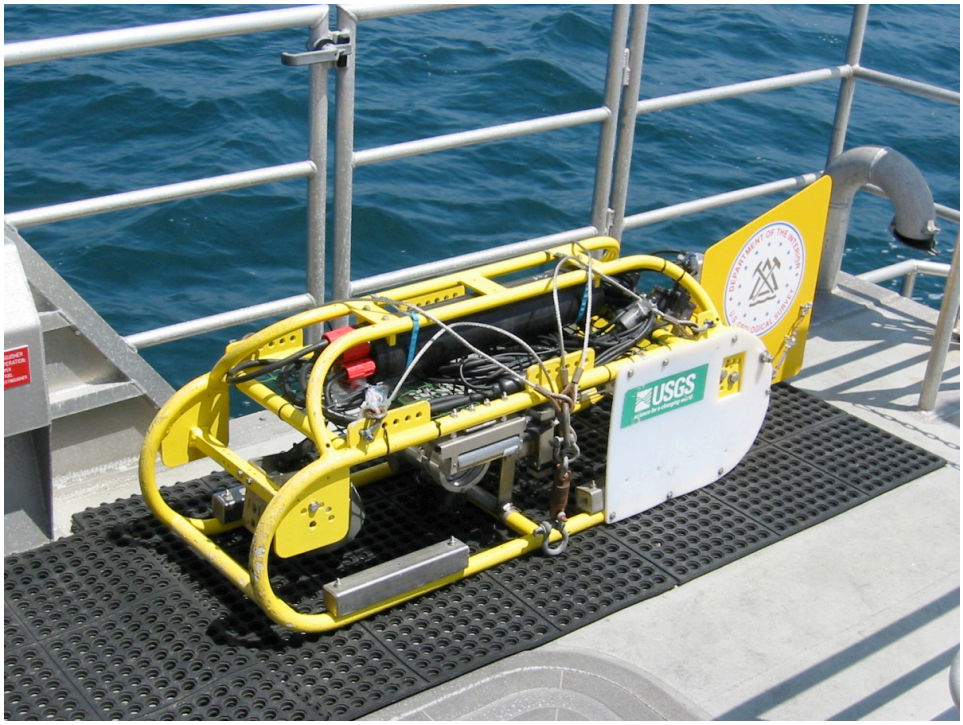

Figure 5–1. Photograph of camera sled used in USGS 2008 ground-truth survey.

substrate, slope, abiotic complexity, biotic complexity, and biotic cover are mandatory. Observations of key geologic features and the presence of key species also are made.

Primary and secondary substrates constitute greater than 50 and 20 percent of the seafloor, respectively, during an observation. The classifications are based on the Wentworth scale, except that the granule and pebble sizes have been grouped together into a class called "gravel," and the clay and silt sizes have been grouped together into a class called "mud." Benthic-habitat complexity, which is divided into abiotic (geologic) and biotic (biologic) components, refers to the visual classification of local geologic features and biota that potentially can provide refuge for both juvenile and adult forms of various species (Tissot and others, 2006).

Sheet 6 contains a smaller, simplified (depth-zone symbology has been removed) version of the seafloor-character map on sheet 5. On this simplified map, the camera-sled tracklines used to ground-truth-survey the sonar data are shown by aligned colored dots, each dot representing the location of a recorded observation. A combination of abiotic attributes (primary- and secondary-substrate compositions, as well as vertical variability) were used to derive the different classes represented on the seafloor-character map (sheet 5); on the simplified map, the derived classes are represented by colored dots. Also on this map are locations of the detailed views of seafloor character, shown by boxes (Boxes A through E); for each view, the box shows the locations (indicated by colored stars) of representative seafloor photographs. For each photograph, an explanation of the observed seafloor characteristics recorded by USGS and NOAA scientists is given. Note that individual photographs often show more substrate types than are reported as the primary and secondary substrate. Organisms, when present, are labeled on the photographs.

The ground-truth survey is designed to investigate areas that represent the full spectrum of high-resolution multibeam bathymetry and backscatter-intensity variation. Figure 5–2 shows that, in the Offshore of Carpinteria map area, the surface is covered predominantly with mixtures of mud and sand. Hard substrates observed in video are either differentially eroded sedimentary-rock outcrops (areas A and E), boulders in the subaqueous delta offshore of Rincon Point (area C), or oil platforms. A video transect across an oil-platform–related pipeline (area D) did not reveal any exposed pipe.

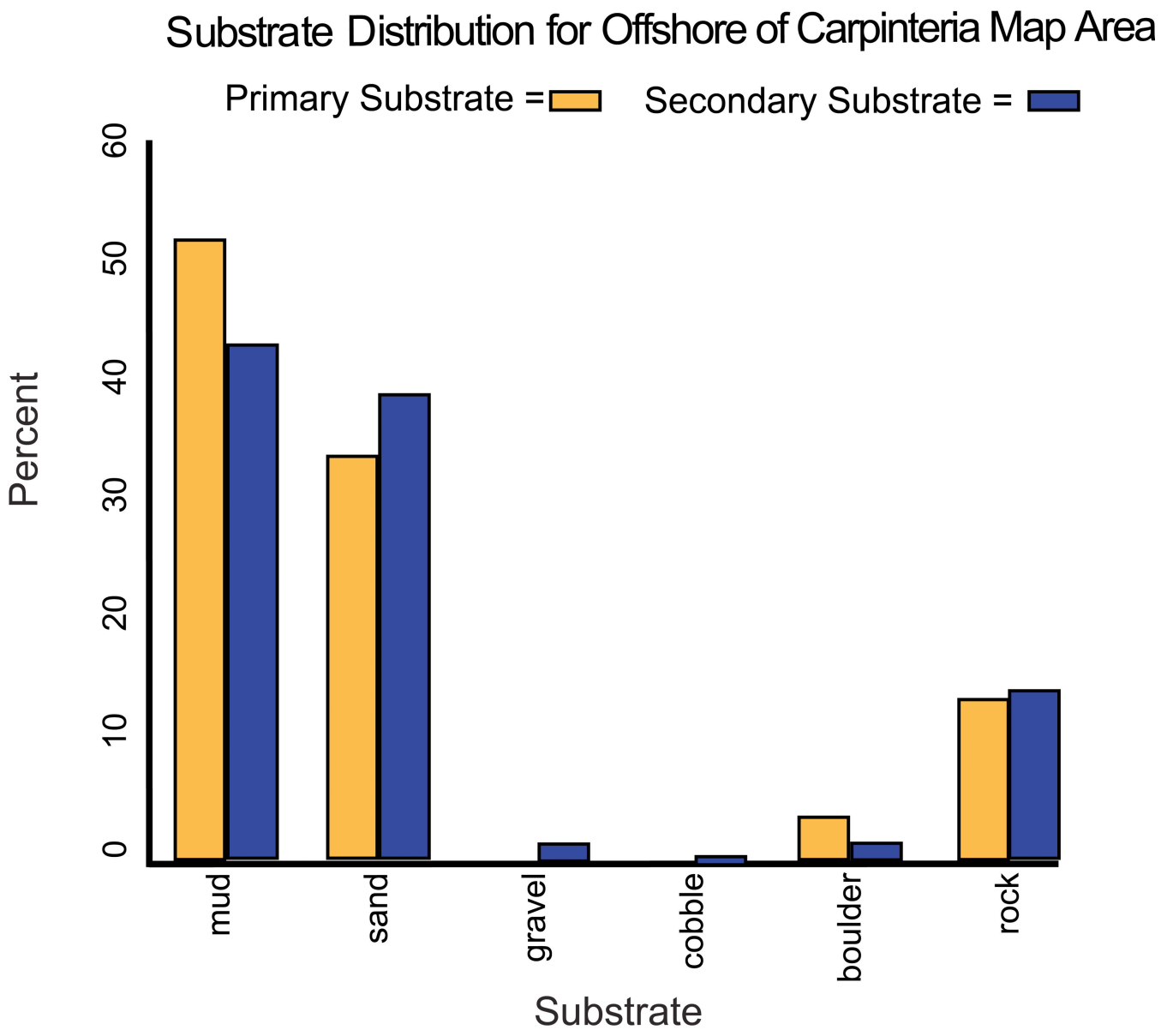

Figure 5–2. Graph showing distribution of primary and secondary substrate determined from video observations in Offshore of Carpinteria map area.

Chapter 6. Potential Marine Benthic Habitat Map of the Offshore of Carpinteria Map Area (Sheet 7)

By H. Gary Greene and Charles A. Endris

The map on sheet 7 shows "potential" marine benthic habitats of the Offshore of Carpinteria map area, representing a substrate type, geomorphology, seafloor process, or any other attribute that may provide a habitat for a specific species or assemblage of organisms. This map, which is based largely on seafloor geology, also integrates information displayed on several other thematic maps of the Offshore of Carpinteria map area. High-resolution sonar bathymetry data, converted to depth grids (seafloor DEMs; sheet 1), are essential to development of the potential marine benthic habitat map, as is shaded-relief imagery (sheet 2), which allows visualization of seafloor terrain and provides a foundation for interpretation of submarine landforms.

Backscatter maps (sheet 3) are also essential for developing potential benthic habitat maps. High backscatter is further indication of "hard" bottom, consistent with interpretation as rock or coarse sediment. Low backscatter, indicative of a "soft" bottom, generally indicates a fine sediment environment. Habitat interpretations are also informed by actual seafloor observations from ground-truth surveying (sheet 6), by seafloor-character maps that are based on video-supervised maximum-likelihood classification (sheet 5), and by seafloor-geology maps (sheet 10). The habitat interpretations on sheet 7 are further informed by the usSEABED bottom-sampling compilation of Reid and others (2006).

Broad, generally smooth areas of seafloor that lack sharp and angular edge characteristics are mapped as "sediment;" these areas may be further defined by various sedimentary features (for example, erosional scours and depressions) and (or) depositional features (for example, dunes, mounds, or sand waves). In contrast, many areas of seafloor bedrock exposures are identified by their common sharp edges and high relative relief; these may be contiguous outcrops, isolated parts of outcrop protruding through sediment cover (pinnacles or knobs), or isolated boulders. In many locations, areas within or around a rocky feature appear to be covered by a thin veneer of sediment; these areas are identified on the habitat map as "mixed" induration (that is, containing both rock and sediment). The combination of remotely observed data (for example, high-resolution bathymetry and backscatter, seismic-reflection profiles) and directly observed data (for example, camera transects, sediment samples) translates to higher confidence in the ability to interpret broad areas of the seafloor.

To avoid any possible misunderstanding of the term "habitat," the term "potential habitat" (as defined by Greene and others, 2005) is used herein to describe a set of distinct seafloor conditions that in the future may qualify as an "actual habitat." Once habitat associations of a species are determined, they can be used to create maps that depict actual habitats, which then need to be confirmed by in situ observations, video, and (or) photographic documentation.

Classifying Potential Marine Benthic Habitats

Potential marine benthic habitats in the Offshore of Carpinteria map area are mapped using the Benthic Marine Potential Habitat Classification Scheme, a mapping-attribute code developed by Greene and others (1999, 2007). This code, which has been used previously in other offshore California areas (see, for example, Greene and others, 2005, 2007), was developed to easily create categories of marine benthic habitats that can then be queried within a GIS or a database. The code contains several categories that can be subdivided relative to the spatial scale of the data. The following categories can be applied directly to habitat interpretations determined from remote-sensing imagery collected at a scale of tens of kilometers to one meter: Megahabitat, Seafloor Induration, Meso/Macrohabitat, Modifier, Seafloor Slope, Seafloor Complexity, and Geologic Unit. Additional categories of Macro/Microhabitat,

Seafloor Slope, Seafloor Complexity, and Geologic Attribute can be applied to habitat interpretations determined from seafloor samples, video, still photographs, or direct observations at a scale of 10 meters to a few centimeters. These two scale-dependent groups of categories can be used together, to define a habitat across spatial scales, or separately, to compare large- and small-scale habitat types.

The six categories and their attribute codes that are used on the Offshore of Carpinteria map are explained in detail below (note, however, that not all categories may be used in a particular map area, given the study objectives, data availability, or data quality); attribute codes in each category are depicted on the map by the letters and, in some cases, numbers that make up the map-unit symbols:

Megahabitat—Based on depth and general physiographic boundaries; used to distinguish features on a scale of tens of kilometers to kilometers. Depicted on map by capital letter, listed first in map-unit symbol; generalized depth ranges are given below.

F = Flank; continental slope, basin and (or) island flanks (200 to 3,000 m)
S = Shelf; continental and island shelves (0 to 200 m)

Seafloor Induration—Refers to substrate hardness. Depicted on map by lower-case letter, listed second in map-unit symbol; may be further subdivided into distinct sediment types, depicted by lower-case letter(s) in parentheses, listed immediately after substrate hardness; multiple attributes listed in general order of relative abundance, separated by slash; queried where inferred.

h = Hard bottom (for example, rock outcrop or sediment pavement)
m = Mixed hard and soft bottom (for example, local sediment cover of bedrock)
s = Soft bottom; sediment cover
(g) = Gravel
(s) = Sand
(m) = Mud, silt, and (or) clay

Meso/Macrohabitat—Related to scale of habitat; consists of seafloor features one kilometer to one meter in size. Depicted on map by lower-case letter and, in some cases, additional lower-case letter in parentheses, listed third in map-unit symbol; multiple attributes separated by slash.

b = Beach, relic (submerged) or shoreline
(b)/p = Pinnacle indistinguishable from boulder
c = Canyon
  c(b) = Bar within thalweg
  c(c) = Curve or meander within thalweg
  c(f) = Fall or chute within thalweg
  c(h) = Canyon head
  c(m) = Canyon mouth
  c(t) = Thalweg
  c(w) = Canyon wall
d = Deformed, tilted and (or) folded bedrock; overhang
e = Exposure; bedrock
f = Flat; floor
g = Gully; channel
h = Hole; depression
l = Landslide; mass movement; rubble
m = Mound; linear ridge
o = Overbank deposit; levee
p = Pinnacle; cone
r = Rill (linear depression on surface formed by subterranean winnowing of sediment)
s = Scarp, cliff, fault, or slump scar
t = Terrace

v = Vegetated (grass- or algae-covered) sediment or rock
w = Dynamic bedform
w(w) = Sediment wave (amplitude, 10 cm to a meter; wave length, tens of meters)
w(d) = Sediment dune (amplitude, tens of meters; wave length, hundreds of meters)
y = Delta; fan

Modifier—Describes texture, bedforms, biology, or lithology of seafloor. Depicted on map by lower-case letter, in some cases followed by additional lower-case letter(s) either after hyphen or in parentheses (or both), following an underscore; multiple attributes separated by slash.

_a = Anthropogenic (artificial reef, breakwall, shipwreck, disturbance)
_a-c = Cable
_a-dd = Dredge disturbance
_a-dg = Dredge groove or channel
_a-dp = Dredge potholes
_a-dm = Dredge mound (disposal)
_a-dp = Dredge pothole
_a-f = Ferry (or other vessel) propeller-wash scour or scar
_a-g = Groin, jetty, rip-rap
_a-m = Marina, harbor
_a-p = Pipeline
_a-s = Support; dock piling, dolphin
_a-td = Trawl disturbance
_a-w = Wreck, ship, barge, or plane
_b = Bimodal (conglomeratic, mixed [gravel, cobbles, and pebbles])
_c = Consolidated sediment (claystone, mudstone, siltstone, sandstone, breccia, or conglomerate)
_d = Differentially eroded
_e = Effusive pit; pockmark
_f = Fracture, joint; faulted
_g = Granite
_h = Hummocky, irregular relief
_i = Interface; lithologic contact
_k = Kelp
_l = Limestone or carbonate rock or structure
_l(a) = Alive reef
_l(d) = Dead reef
_l(l) = Linear reef
_l(p) = Patch reef
_l(pr-a) = Aggregated patch reef
_l(pr-i) = Individual patch reef
_l(r) = Reef rubble
_l(s-g) = Spur and groove
_m = Massive sedimentary bedrock
_o = Outwash
_p = Pavement
_r = Ripple (amplitude, greater than 10 cm)
_s = Scour (current or ice; direction noted)
_u = Unconsolidated sediment
_v = Volcanic rock

_w = Wall

Seafloor Slope—Denotes slope, typically calculated from XYZ high-resolution bathymetry data. Depicted on map by number, listed after modifier.

1 = Flat (0º–5º)
2 = Sloping (5º–30º)
3 = Steeply sloping (30º–45º)
4 = Vertical or near vertical (45º–90º)
5 = Overhanging (more than 90º)
6 = Unknown

Geologic Attribute—Describes additional geologic features seen in video, still photographs, or other types of direct observations. Depicted on map by lower-case letter(s) in parentheses, preceded by an asterisk.

*(a) = Anthropogenic (for example, cable, pipeline, disturbance)
    *(a-d) = Dredge track, pit, or mound
*(b) = Boulder
*(d) = Deformed, faulted, or folded
*(e) = Exposure, bedrock (sedimentary, igneous, or metamorphic)
    *(e-r) = Rough bedrock surface
*(f) = Fan or apron
*(g) = Gravel
*(j) = Joint, crack, crevice, overhang (differentially eroded)
*(l) = Limestone, carbonate deposit
*(m) = Mud, silt, or clay
*(q) = Coquina (shell hash)
*(r) = Rubble
*(s) = Sand
*(t) = Flat, terracelike seafloor, including sedimentary pavement
*(u) = Undulating surface, hummocky
    *(u-r) = Ripple
    *(u-s) = Scour
    *(u-w) = Sediment wave
*(y) = Barnacle or plate

Examples of Attribute Coding

To illustrate how these attribute codes can be used to describe remotely sensed data, the following examples are given:

Ssc(h)_u2/4 = Canyon head that indents shelf and has smooth, soft, gently sloping, sedimentary walls, locally cropping out as steep (near vertical) scarps (10 to 100 m).

Ssf_u1 = Flat to gently sloping shelf that has soft, unconsolidated sediment (10 to 150 m).

Fhe_m/c = Continental slope that has hard sedimentary (sandstone) bedrock exposures locally and smooth to moderately irregular relief (less than 1 m to 3 m high); exposures often covered with sediment (200 to 2,500 m).

Ssm_a/u*(q) = Soft, unconsolidated sediment and shell-hash mound, adjacent to oil platform (anthropogenic).

Map Area Habitats

The Offshore of Carpinteria map area is mainly flat with local small areas of low-relief sedimentary-bedrock exposures and a coarse-grained delta offshore of Rincon Point. Backscatter data (sheet 3) show that most of the area is underlain by "soft" materials, consistent with the interpretation that unconsolidated sediment dominates the habitat types in the map area. Habitat types range from predominantly soft, unconsolidated sediment (sand and mud to gravel) to small areas of hard bedrock exposures and coarse-grained sediment (gravel to boulders). In some places, rock exposures and adjacent sediment combine to produce a hard-soft mixed habitat type. Twenty-four potential marine benthic habitat types are delineated in the map area, all on the continental shelf ("Shelf" megahabitat). The meso- and macrohabitats include bedrock exposures, terraces, delta, and carbonate mounds, with pockmarks, depressions, and anthropogenic features as modifiers.

Although much of the map area is flat and appears to be fairly homogeneous, it also contains three locally exposed outcrops of differentially eroded sedimentary rock; these include overhangs and crevices, which are potentially good habitat for rockfish (*Sebastes* spp.). Significant anthropogenic features associated with oil production, such as platforms, pipelines, and shell mounds beneath platforms, as well as jetties and groins, also produce artificial habitats for rockfish. Small areas of carbonate mounds and pavement provide hard habitat on the soft, sediment-covered shelf and provide substrate for encrusting and sessile organisms.

The soft, unconsolidated sediment habitat, which includes pockmarks and carbonate mounds, covers 135.67 km^2 of the map area, representing 95.5 percent of all the potential habitat types identified. Sediment-covered bedrock, which includes the hard-soft mixed habitat type, covers 2.15 km^2 (1.5 percent). Hard bedrock exposures cover 1.21 km^2 (0.9 percent), whereas anthropogenic features cover about 3.06 km^2 (<2.2 percent).

Chapter 7. Subsurface Geology and Structure of the Offshore of Carpinteria Map Area and the Santa Barbara Channel Region (Sheets 8 and 9)

By Samuel Y. Johnson, Eleyne L. Phillips, Andrew C. Ritchie, Florence L. Wong, Ray W. Sliter, Amy E. Draut, and Patrick E. Hart

The seismic-reflection profiles presented on sheet 8 provide a third dimension, depth, to complement the surficial seafloor-mapping data already presented (sheets 1 through 7) for the Offshore of Carpinteria map area. These data, which are collected at several resolutions, extend to varying depths in the subsurface, depending on the purpose and mode of data acquisition. The seismic-reflection profiles (sheet 8) provide information on sediment character, distribution, and thickness, as well as potential geologic hazards, including active faults, areas prone to strong ground motion, and tsunamigenic slope failures. The information on faults provides essential input to national and state earthquake-hazard maps and assessments (for example, Petersen and others, 2008).

The maps on sheet 9 show the following interpretations, which are based on the seismic-reflection profiles on sheet 8: the thickness of the uppermost sediment unit; the depth to base of this uppermost unit; and both the local and regional distribution of faults and earthquake epicenters (data from Heck, 1998; Minor and others, 2009; Jennings and Bryant, 2010; Southern California Earthquake Data Center, 2010).

Data Acquisition

Most profiles displayed on sheet 8 (figs. 1, 2, 3, 4, 5, 6, 8, 9, 10, 12) were collected in 2007 on U.S. Geological Survey (USGS) cruise Z–3–07–SC (Sliter and others, 2008). Single-channel seismic-reflection data were acquired using two different sources, the SIG 2Mille minisparker (figs. 3, 10, 12) and the EdgeTech 512 chirp (figs. 1, 2, 4, 5, 6, 8, 9). The SIG minisparker system used a 500-J high-voltage electrical discharge fired at 1 to 4 times per second, which, at normal survey speed of 4 to 4.5 nautical miles/hour, gives a data trace every 0.5 to 2.0 meters of lateral distance covered. The data were digitally recorded in standard SEG-Y 32-bit floating-point format, using Triton Subbottom Logger (SBL) software that merges seismic-reflection data with differential GPS-navigation data. The EdgeTech 512 chirp subbottom-profiling system consists of a source transducer and an array of receiving hydrophones housed in a 500-lb fish towed at a depth of several meters below the sea surface. The swept-frequency chirp source signal was 500 to 4,500 Hz and 50 ms in length, and it was recorded by hydrophones located on the bottom of the fish. After the survey, a short-window (20 ms) automatic gain control algorithm was applied to both the chirp and minisparker data, and a 160- to 1,200-Hz bandpass filter was applied to the minisparker data. These high-resolution data can resolve geologic features that are a few meters thick (small-scale features) to subbottom depths of as much as a few hundred meters.

Figures 7 and 11 on sheet 8 show deep-penetration, migrated, multichannel seismic-reflection profiles collected in 1985 by the WesternGeco on cruise W–40–85–SC. These profiles and other similar data were collected in many areas offshore of California in the 1970s and 1980s when the area was considered a frontier for oil and gas exploration. Much of these data have been publicly released and are now archived at the U.S. Geological Survey National Archive of Marine Seismic Surveys (U.S. Geological Survey, 2009). These data were acquired using a large-volume air-gun source at a frequency range of 3 to 40 Hz and recorded with a multichannel hydrophone streamer about 2 km long. Shot

spacing was about 30 m. These data can resolve geologic features that are 20 to 30 m thick to subbottom depths of about 4 km.

Seismic-Reflection Imaging of the Continental Shelf

Sheet 8 shows seismic-reflection profiles in the Offshore of Carpinteria map area that document a broad, relatively shallow (less than 40 m) wave-cut shelf. This shelf is relatively flat (less than 0.5°) and mostly underlain by variably thick (0 m to about 30 m) upper Pleistocene and Holocene sediments (Dahlen, 1992; Slater and others, 2002; Sommerfield and others, 2009), much of which was deposited in the last about 21,000 years during the about 125-m sea-level rise that followed glaciation and the last major sea-level lowstand. Sea-level rise after the Last Glacial Maximum (LGM) was rapid (about 9 to 11 m per thousand years) until about 7,000 years ago, at which time it slowed considerably (to about 1 m per thousand years) (Fairbanks, 1989; Fleming and others, 1998; Lambeck and Chappell, 2001; Peltier and Fairbanks, 2006). Local relief on the shelf is associated with bedrock uplifts (see sheet 10).

In the high-resolution seismic-reflection profiles on sheet 8 (figs. 1, 2, 3, 4, 5, 6, 8, 9, 10, 12), sediments deposited during this latest Pleistocene and Holocene sea-level rise (shaded blue in profiles) are typically characterized by parallel, low- to moderate-amplitude, moderate- to high-frequency, continuous to moderately continuous reflections (terminology from Mitchum and others, 1977). An upward decrease in reflection amplitude is seen on many profiles. Because the shelf was partly emergent during the postglacial period of rising sea level, the lower part of the blue-shaded unit may locally consist of marginal marine deposits. These strata were covered by nearshore and shelf sediments as sea level rose and the shoreline migrated both landward and upward. The upper part of this unit consists primarily of shelf deposits that are similar to the sediments found on the shelf today.

The presence and continuity of seismic reflections in the blue-shaded unit on many profiles is obscured by interstitial gas within the sediments. This effect has been referred to as “gas blanking,” “acoustic turbidity,” or “acoustic masking” (Hovland and Judd, 1988; Fader, 1997). The gas scatters or attenuates the acoustic energy, preventing penetration. Not surprisingly, this effect is especially prevalent along the projected trace of the Rincon Anticline (see figs. 4, 6, 8 on sheet 8), which hosts several actively producing hydrocarbon fields (see, for example, Barnum, 1998).

On most profiles on sheet 8, the base of the latest Pleistocene and Holocene (post-LGM) depositional unit is a flat to concave angular unconformity, characterized by a high-amplitude reflection. Post-LGM sediment onlapping of local uplifts is common (figs. 2, 10). Sediment-covered wave-cut platforms and risers (see, for example, Kern, 1977) are imaged at the base of the unit on some profiles, most commonly at depths of about 23 m (fig. 4) and also about 35 to 40 m (fig. 2). Given uplift rates from nearby coastal terraces (Trecker and others, 1998; Keller and Gurrola, 2000, their fig. 6), these depths are consistent with formation during late oxygen-isotopic stage 3, about 25 to 40 ka. Alternatively, they could also have formed during the post-LGM transgression. Post-LGM sea-level rise and landward shoreline migration were not steady but, rather, were characterized by periods of relative stability and rapid submergence (see, for example, Peltier, 2005; Stanford and others, 2011). For example, sea level rose about 20 m in 200 to 500 years during meltwater pulse 1A, about 14,000 years ago. Such pulses rapidly submerge wave-cut platforms, shorelines, and shoreline angles (Kern, 1977), thereby increasing the potential for their preservation.

Redin and others’ (1998) cross section shows that the folding of strata beneath the post-LGM unconformity extends upward from the Miocene Monterey Formation into the Pliocene and Pleistocene Pico Formation.

Geologic Structure and Recent Deformation

Seismic-reflection profiles in the Offshore of Carpinteria map area (sheet 8) show significant folding and three important active faults. The blind-thrust or blind-reverse, east-west-striking, north-dipping Pitas Point Fault crosses the southern part of the map area, where it is expressed by a narrow (about 250- to 300-m-wide), south-dipping monocline in the shallow subsurface (Johnson and others, 2013). Deeper industry seismic-reflection profiles (figs. 7, 11 on sheet 8) reveal at least two other north-dipping blind-reverse faults and the Rincon Anticline in the hanging wall of the Pitas Point Fault, consistent with the cross section of Redin and others (1998). One of these north-dipping structures, the east-west-striking Red Mountain Fault, crosses the shoreline between Rincon Point and Punta Gorda (fig. 1–2; see also, Jackson and Yeats, 1982; Tan and others, 2003a), about 6 km north of the Pitas Point Fault. This fault is considered active, mainly on the basis of offset marine terraces onshore (Lajoie and others, 1982; Trecker and others, 1998; Wills and others, 2008). Offshore, the trace of the Red Mountain Fault follows a linear, about 300-m-long, low-relief (20-cm-high) scarp on the rocky submarine extension of Rincon Point. The Red Mountain Fault bifurcates about 6 km west of the coast into a north-dipping south strand and a south-dipping north strand, forming the boundaries of a Neogene bedrock uplift (figs. 2, 10 on sheet 8; see also, sheet 10). The Red Mountain Fault also has a significant control on sediment thicknesses (see sheet 9).

The east-west-striking Rincon Creek Fault, which crosses the shoreline 3 km north of the Red Mountain Fault, forms the north edge of a seafloor bedrock (the steeply dipping Monterey Formation) uplift for more than 3 km. This fault is crossed by only one seismic-reflection profile in the Offshore of Carpinteria map area (fig. 1 on sheet 8), where it is seen to juxtapose bedrock of the Monterey Formation with gently dipping Pleistocene strata of the Santa Barbara and Casitas Formations in the shallow subsurface, forming the southern margin of a Quaternary sedimentary basin. The Rincon Creek Fault has been interpreted as a steeply south-dipping splay fault that branches off of the Red Mountain Fault at depth (Jackson and Yeats, 1982; Redin and others, 1998, 2004). Near the west edge of the map area, both the trace of the Rincon Creek Fault and the margin of this basin appear to be offset about 1,000 m to the south by a transfer zone that may trend north-south.

Folds in the Neogene strata that are present between these three faults (Pitas Point Fault, Red Mountain Fault, Rincon Creek Fault) have varying wavelengths, amplitudes, and lengths. Longer structures such as the broad syncline north of the Red Mountain Fault (figs. 3, 5 on sheet 8) can be traced for as long as 13 km (see sheet 10), whereas folds associated with local deformation (fig. 3 on sheet 8) commonly die out within a few kilometers.

The regional pattern of faults and earthquakes occurring between 1932 and 2010 that have inferred or measured magnitudes greater than 2.0 are shown on Map C on sheet 9. Although locations have been provided by the CalTech network since 1932, significantly greater precision began in 1969 with installation of a USGS seismographic network (see, for example, Lee and Vedder, 1973; Sylvester, 2001; Southern California Earthquake Data Center, 2010). Epicentral data indicate that seismicity in the eastern and central Santa Barbara Channel is characterized by earthquake swarms, relatively frequent minor earthquakes, and infrequent major earthquakes.

Three significant earthquakes affected the Santa Barbara Channel area in 1812, 1857, and 1925, prior to the time covered by the Southern California Earthquake Data Center (2010) catalog; however, locations in the northern Santa Barbara Channel have been reported (Sylvester and others, 1970) for both the 1925 event (M6.3) and the largest earthquake (~M5.5, 7/1/1941), which is shown on Map C on sheet 9. In addition, Sylvester and others (1970) documented a swarm of 62 earthquakes (M2.5–M5.2) that occurred between 6/26/1968 and 8/3/1968, which also were located 10 to 15 km south (offshore) of Santa Barbara. The largest event in the Offshore of Carpinteria map area (~M5.5) occurred on 7/1/1941 about 6 km south of Summerland.

Thickness and Depth of Uppermost Pleistocene and Holocene Deposits

Maps on sheet 9 show the thickness and the depth to base of uppermost Pleistocene and Holocene (post-LGM) deposits both for the Offshore of Carpinteria map area (Maps A, B) and, to establish regional context, for a larger area (about 115 km of coast) that extends from the vicinity of Hueneme Canyon northwest to the Refugio Beach area (Maps D, E). To make these maps, water bottom and depth to base of the LGM horizons were mapped from seismic-reflection profiles using Seisworks software. The difference between the two horizons was exported from Seisworks for every shot point as XY coordinates (UTM zone 11) and two-way travel time (TWT). The thickness of the post-LGM unit (Maps B, E) was determined by applying a sound velocity of 1,600 m/sec to the TWT, resulting in thicknesses as great as 65 m. The thickness points were interpolated to a preliminary continuous surface, overlaid with zero-thickness bedrock outcrops (see sheet 10), and contoured (Wong and others, 2012). Data within Hueneme Canyon were excluded from the contouring because the seismic-reflection data are too sparse to adequately image the highly variable changes in sediment thickness that characterize the canyon (Maps D, E).

Several factors required manual editing of the preliminary thickness maps to make the final product. The Red Mountain Fault Zone, Pitas Point Fault, and Oak Ridge Fault disrupt the sediment sequence in the region (Maps D, E on sheet 9). The data points also are dense along tracklines (about 1 m apart) and sparse between tracklines (1–2 km apart), resulting in contouring artifacts. To incorporate the effect of the faults, to remove irregularities from interpolation, and to reflect other geologic information and complexity, the resulting interpolated contours were modified. Contour modifications and regridding were repeated several times to produce the final regional sediment-thickness map (Wong and others, 2012).

The depth-to-base data available from Seisworks were similarly processed and contoured; however, this preliminary data set was set aside in favor of a surface determined by subtracting the modified thickness data from multibeam bathymetry collected separately (see sheet 1) and using 1,500 m/sec for TWT in the water column. The depth of this surface in the Hueneme Canyon to Refugio Beach area ranges from 12 to 190 m (Map D on sheet 9; see also, Wong and others, 2012).

Five different "domains" of sediment thickness, which are bounded either by faults or by Hueneme Canyon, are recognized on the regional maps (Maps D, E on sheet 9): (1) north of the south strand of the Red Mountain Fault Zone; (2) between the south strand of the Red Mountain Fault Zone and the Pitas Point Fault; (3) between the Pitas Point and Oak Ridge Faults; (4) between the Oak Ridge Fault and Hueneme Canyon; and (5) south of Hueneme Canyon. Table 7–1 shows the area of these five domains, along with estimates of their mean sediment thickness and total sediment volume. These data highlight the contrast among three general zones of sediment thickness: (1) the uplifted, sediment-poor Santa Barbara shelf (domain 1; mean sediment thickness of 3.5 m); (2) a transitional zone (domain 2; mean sediment thickness of 18.0 m); and (3) the subsiding, sediment-rich delta and shelf offshore of the Ventura and Santa Clara Rivers and Calleguas Creek (domains 3, 4, and 5; mean sediment thicknesses of 39.3, 38.9, and 28.3 m, respectively).

In the Offshore of Carpinteria map area, thickness data (Map B on sheet 9) reveal that the post-LGM section north of the south strand of the Red Mountain Fault ranges from 0 m to 17 m thick but has a mean thickness of just 5.1 m (table 7–1). The thickest accumulations are in a gentle trough between the uplifts associated with the Red Mountain and Rincon Creek Faults (fig. 1 on sheet 8; see also, sheet 10). The origin of this trough could be either structural or erosional (or both); although it is spatially related to a broad syncline (figs. 1, 2 on sheet 8), it also could represent the axis of a lowstand paleodrainage system.

Mean sediment thickness increases substantially (from 5.1 to 19.2 m) in the domain between the south strand of the Red Mountain Fault and the Pitas Point Fault, with thickness increasing parallel to

the coast in the nearshore and perpendicular to the coast (parallel to the two faults) farther offshore. This southward thinning is consistent with deposition over a growing structural arch above the Pitas Point Fault, an inference confirmed with noted northward sediment thinning and pinch out on seismic-reflection profiles (fig. 10 on sheet 8).

Mean sediment thickness also increases substantially (from 19.2 to 44.0 m) across the narrow Pitas Point Fault monocline, an observation consistent with the young structural relief along this structure, as noted by Johnson and others (2013).

Table 7–1. Area, sediment-thickness, and sediment-volume data for California's State Waters in Santa Barbara Channel region, between Refugio Beach and Hueneme Canyon areas (domains 1–5), as well as in Offshore of Carpinteria map area and in three areas within map area.

[Data from within Hueneme Canyon were not included in this analysis]

Regional sediment-thickness domains in Santa Barbara Channel region			
	Area (km^2)	**Mean sediment thickness (m)**	**Sediment volume (10^6 m^3)**
(1) Refugio Beach to south strand of Red Mountain Fault Zone	357.8	3.5	1,266
(2) South strand of Red Mountain Fault Zone to Pitas Point Fault	67.1	18.0	1,205
(3) Pitas Point Fault to Oak Ridge Fault	68.6	39.2	2,688
(4) Oak Ridge Fault to Hueneme Canyon	75.4	38.9	2,933
(5) South of Hueneme Canyon	53.9	28.3	1,527
Sediment thicknesses in Offshore of Carpinteria map area			
Entire Offshore of Carpinteria map area	108.5	12.7	1,380
Map area north of south strand of Red Mountain Fault Zone	55.8	5.1	283
Map area between south strand of Red Mountain Fault Zone and Pitas Point Fault	49.3	19.2	944
Map area south of Pitas Point Fault	3.5	44.0	153

Chapter 8. Geologic and Geomorphic Map of the Offshore of Carpinteria Map Area (Sheet 10)

By Samuel Y. Johnson, Andrew C. Ritchie, Gordon G. Seitz, and Carlos I. Gutierrez

Geologic and Geomorphic Summary

Marine geology and geomorphology was mapped in the Offshore of Carpinteria map area from approximate Mean High Water (MHW) to the 3-nautical-mile limit of California's State Waters. MHW is defined at an elevation of 1.33 m above the North American Vertical Datum of 1988 (NAVD 88) (Weber and others, 2005). Offshore geologic units were delineated on the basis of integrated analyses of adjacent onshore geology with multibeam bathymetry and backscatter imagery (sheets 1, 2, 3), seafloor-sediment and rock samples (Reid and others, 2006), digital camera and video imagery (sheet 6), and high-resolution seismic-reflection profiles (sheet 8).

The onshore geology was compiled from Dibblee (1986), Tan and others (2003a,b), Tan and Clahan (2004), and Minor and others (2009). Unit ages, which are from these sources, reflect local stratigraphic relations.

The offshore part of the map area largely consists of a relatively shallow (less than about 45 m deep), gently offshore-dipping (less than 1°) shelf underlain by sediments derived primarily from relatively small coastal watersheds that drain the Santa Ynez Mountains. Shelf deposits are primarily sand (unit Qms) at water depths less than about 25 m and, at depths greater than about 25 m, are the more fine-grained sediments (very fine sand, silt, and clay) of unit Qmsf. The boundary between units Qms and Qmsf is based on observations and extrapolation from sediment sampling (see, for example, Reid and others, 2006) and camera ground-truth surveying (see sheet 6). It is important to note that the boundary between units Qms and Qmsf should be considered transitional and approximate and is expected to shift as a result of seasonal- to annual- to decadal-scale cycles in wave climate, sediment supply, and sediment transport.

Coarser grained deposits (coarse sand to boulders) of unit Qmsc, which are recognized on the basis of their moderate seafloor relief and high backscatter (sheet 3), as well as camera observations (sheet 6) and sampling (Reid and others, 2006; Barnard and others, 2009), are found locally in water depths less than about 15 m, except offshore of Rincon Point where they extend to depths of about 21 m. The largest Qmsc deposits are present at the mouths of Rincon Creek and Toro Canyon Creek. The convex seafloor relief of these coarse-grained deposits suggests that they are wave-winnowed lags that armor the seafloor and are relatively resistant to erosion. The sediments may, in part, be relict, having been deposited in shallower marine (or even alluvial?) environments at lower sea levels in the latest Pleistocene and Holocene; this seems especially likely for the arcuate lobe of unit Qmsc that extends 1,700 m offshore from Rincon Point. The Qmsc deposits offshore of Toro Canyon Creek are found adjacent to onshore alluvial and alluvial fan deposits (Minor and others, 2009) and, thus, may have formed as distal-alluvial or fan-delta facies of that system.

Offshore bedrock exposures are assigned to the Miocene Monterey Formation (unit Tm) and the Pliocene and Pleistocene Pico Formation (unit QTp), primarily on the basis of extrapolation from the onshore mapping of Tan and others (2003a,b), Tan and Clahan (2004), and Minor and others (2009), as well as the cross sections of Redin and others (1998, 2004) that are constrained by industry seismic-reflection data and petroleum well logs. Where uncertainty exists, bedrock is mapped as an undivided unit (QTbu). These rocks are exposed in structural highs that include the Rincon Anticline and uplifts bounded by the Rincon Creek Fault and by the north and south strands of the Red Mountain Fault.

Bedrock is, in some places, overlain by a thin (less than 1 m?) veneer of sediment, recognized on the basis of high backscatter, flat relief, continuity with moderate- to high-relief bedrock outcrops, and

(in some cases) high-resolution seismic-reflection data; these areas, which are mapped as composite units Qms/Tm, Qms/QTbu, or Qms/QTp, are interpreted as ephemeral sediment layers that may or may not be continuously present, whose presence or absence is a function of the recency and intensity of storm events, seasonal and (or) annual patterns of sediment movement, or longer term climate cycles.

Two offshore anthropogenic units also are present in the map area, each related to offshore hydrocarbon production. The first (unit af) consists of coarse artificial fill associated with construction of the Rincon Island petroleum-production facility near the east edge of the map area. The second (unit pd) consists of coarse artificial fill mixed with sediment and shell debris, mapped in outcrops surrounding Rincon Island and at the locations of former oil platforms "Heidi," "Hope," "Hazel," and "Hilda" from the Summerland and Carpinteria oil fields (Barnum, 1998). The Monterey Formation is the primary petroleum-source rock in the Santa Barbara Channel, and the Pico Formation is one of the primary petroleum reservoirs.

The Offshore of Carpinteria map area is in the Ventura Basin, in the southern part of the Western Transverse Ranges geologic province, which is north of the California Continental Borderland (Fisher and others, 2009). This province has undergone significant north-south compression since the Miocene, and recent GPS data suggest north-south shortening of about 6 to 10 mm/yr (Larson and Webb, 1992; Donnellan and others, 1993). The active, east-west-striking, north-dipping Pitas Point Fault (a broad zone that includes south-dipping reverse faults), Red Mountain Fault, and Rincon Creek Fault are some of the structures on which this shortening occurs (see, for example, Jackson and Yeats, 1982; Sorlien and others, 2000; Fisher and others, 2009). This fault system, in aggregate, extends for about 100 km through the Ventura and Santa Barbara Basins and represents an important potential earthquake hazard (see, for example, Fisher and others, 2009).

Table 8–1. Areas and relative proportions of offshore geologic map units in Offshore of Carpinteria map area.

Map Unit	Area (m^2)	Area (km^2)	Percent of total area
af	19,072	0.02	0.02
pd	115,964	0.12	0.09
Qms	53,265,971	53.27	42.33
Qmsc	3,016,954	3.02	2.40
Qmsf	61,782,162	61.78	49.09
Qms/QTbu	291,902	0.29	0.23
Qms/QTp	3,956,048	3.96	3.14
Qms/Tm	2,388,193	2.39	1.90
QTp	707,832	0.71	0.56
Tm	298,547	0.30	0.24
TOTAL	125,842,645	125.86	100.00

DESCRIPTION OF MAP UNITS

OFFSHORE GEOLOGIC AND GEOMORPHIC UNITS

[Note that, where older units (typically, bedrock) are overlain by thin (<1 m thick) Quaternary deposits, composite units are mapped. These composite units, which are shown with gray or white stipple pattern on older unit, are designated by composite label indicating both overlying sediment cover and lower (older) unit, separated by slash (for example, Qms/Tm indicates that thin sheet of Qms overlies Tm)]

af **Artificial fill (late Holocene)**—Rock, sand, and mud; placed, dredged, and (or) modified by human activity; includes coarse construction debris adjacent to Rincon Island

pd **Oil-platform debris (late Holocene)**—Mixed construction material, coarse sediment, and shell debris surrounding Rincon Island and locations of former oil platforms "Heidi," "Hope," "Hazel," and "Hilda"

Qms **Marine nearshore and shelf deposits (late Holocene)**—Predominantly sand; ripple marks common. Found on gently seaward-dipping (less than 1°) surface that extends from shoreline to water depths of about 25 m

Qmsc **Coarse-grained marine nearshore and shelf deposits (late Holocene)**—Predominantly sand to boulders; found on gently seaward-dipping (less than 1°) surface in water depths typically less than about 15 m, except offshore of Rincon Point where it extends to depth of about 21 m. Recognized primarily on basis of high backscatter and low to moderate relief. Two largest exposures are at mouths of Rincon Creek and Toro Canyon Creek

Qmsf **Fine-grained marine shelf deposits (late Holocene)**—Predominantly mud, very fine sand, and silt; commonly bioturbated; found on gently seaward-dipping (less than 1°) surface at depths greater than about 25 m

QTp **Pico Formation (Pleistocene and Pliocene)**—Claystone, siltstone, sandstone, and conglomerate; locally overlain by pebbles, cobbles, and boulders. Stippled areas (composite unit Qms/QTp) indicate where thin sheets of Qms overlie unit. Note that, to east in Offshore of Ventura map area, the Pico Formation is considered to be Pliocene only (Tan and others, 2003a; Tan and Clahan, 2004)

QTbu **Bedrock, undivided (Pleistocene, Pliocene, and Miocene)**—Consists of undivided strata of the Pico, Sisquoc, and Monterey Formations. Mapped only as part of composite unit Qms/QTbu, where thin sheets of Qms overlie unit

Tm **Monterey Formation (Miocene)**—Predominantly well-bedded siliceous and calcareous mudstone and shale. Stippled areas (composite unit Qms/Tm) indicate where thin sheets of Qms overlie unit

ONSHORE GEOLOGIC AND GEOMORPHIC UNITS

[Units are compiled from Dibblee (1986), Tan and others (2003a,b), Tan and Clahan (2004), and Minor and others (2009); unit ages, which are derived from these sources, reflect local stratigraphic relations]

af **Artificial fill (late Holocene)**—Engineered and (or) nonengineered

Qb **Beach deposits (late Holocene)**—Unconsolidated, loose, fine- to coarse-grained sand; well sorted. Mapped in coastal band from shoreline to highest elevation of swash zone

Qes **Coastal-estuarine deposits (late Holocene)**—Locally organic-rich clay, silt, and subordinate amounts of sand. Mapped primarily in tidally influenced environments at El Estero (salt marsh west of Carpinteria)

Qa **Channel alluvium (late Holocene)**—Unconsolidated sediments, primarily pebble to boulder

gravel, in floors and banks of modern stream channels. Commonly incised as much as 5 m into alluvial deposits of associated floodplain (unit Qyf)

Qf **Alluvial fan deposits (late Holocene)**—Moderately to poorly sorted and bedded gravel, sand, silt, and clay. Age is indicated by historical inundation or presence of youthful braid bars and distributary channels

Qyf **Alluvial fan deposits (Holocene)**—Moderately to poorly sorted and moderately to poorly bedded sandy clay, with some silt and gravel; deposited by streams emanating from mountain canyons onto piedmonts and alluvial valley floors; deposits originate as debris flows, hyperconcentrated mudflows, or braided stream flows

Qymp **Paralic deposits of Sea Cliff marine terrace (Holocene)**—Marine, fossiliferous gravel, sand, and silt; semiconsolidated sand; 1,800 to 5,800 yr old (Lajoie and others, 1982, 1991)

Qyd **Debris-flow deposits (Holocene and late Pleistocene)**—Massive, weakly consolidated rock-debris breccia; derived from upslope rock units. Mainly located along lower flanks of Santa Ynez Mountains

Qls **Landslide deposits (Holocene and late and middle Pleistocene)**—Deposits of diverse slope-movement processes, ranging from poorly sorted and disrupted mixtures of rock fragments and soil to relatively intact bedrock slump blocks. Largest landslide deposits may be as thick as 60 m

Qomp **Paralic deposits of Punta Gorda marine terrace (late Pleistocene)**—Weakly to moderately consolidated, variably stratified, fossiliferous gravel, sand, and silt; deposited as marine intertidal, beach, and estuarine deposits and overlying nonmarine eolian, alluvial, and colluvial deposits. Marine-terrace deposits rest on elevated marine wave-cut platforms and form single terraces or flights of terraces that range in elevation from 10 to 90 m (30–300 ft) and in age from 105,000 (oxygen-isotope substage 5c) to 45,000 (substage 3a) years old

Qoa2 **Alluvial deposits (late Pleistocene)**—Weakly consolidated, stratified silt, sand, and gravel; forms low, rounded, moderately dissected terraces and piedmont alluvial fans. Present at elevations higher than modern coastal-piedmont surface

Qoa1 **Older alluvial deposits (late and middle Pleistocene)**—Moderately consolidated, crudely stratified, poorly sorted sand and sandstone, gravel, conglomerate, and breccia, as well as rare interbeds of clay, silt, and mudstone; makes up proximal to distal facies of alluvial fans shed from Santa Ynez Mountains. Unit forms dissected, gently south-sloping, elevated terraces, interfluvial caps, and other erosional remnants as thick as 35 m

Qc **Colluvium (Pleistocene)**—Variably consolidated silt, sand, clay, and gravel

Qca **Casitas Formation (late and middle Pleistocene)**—Nonmarine, moderately to well-consolidated siltstone and silt, sandstone and sand, and conglomerate and gravel; deposited mainly as alluvium, likely shed from Santa Ynez Mountains. Conglomerate and gravel contain greater percentage of Sespe Formation–derived clasts than older alluvial deposits (unit Qoa1) mapped nearby

Qsb **Santa Barbara Formation (middle and early Pleistocene)**—Chiefly marine, friable, bioturbated and massive sandstone; pale gray, buff, and tan; includes subordinate amounts of interbeds and intervals of shale, siltstone, and silty to clayey sandstone. Contains diverse assemblage of marine invertebrate fossils. Rare conglomeratic lenses become more common upsection, and uppermost part of unit locally interfingers with nonmarine conglomerates of older alluvial deposits (unit Qoa1) or the Casitas Formation (unit Qca)

QTp **Pico Formation, undivided (Pleistocene and Pliocene)**—Claystone, siltstone, and sandstone; locally contains pebbles. Note that, to east in Offshore of Ventura map area, the Pico Formation is considered to be Pliocene only (Tan and others, 2003a; Tan and Clahan, 2004)

Tpsc **Lower sandstone and conglomerate unit (Pliocene)**

Tsq **Sisquoc Formation (early Pliocene and late Miocene)**—Marine, tan- to white-weathering, diatomaceous mudstone and shale, conglomerate, and subordinate amounts of dolomite. Unit is distinguished by thick beds of conglomerate containing angular clasts (commonly as much as 1 m across; some blocks as large as 10 m) derived from the Monterey Formation. Both base and top of unit consist of erosional unconformities

Tm **Monterey Formation, undivided (Miocene)**—Marine, predominantly well-bedded, siliceous and calcareous mudstone and shale, with subordinate amounts of porcelanite and dolomite. The Monterey Formation is divided into subunits that are distinguished on basis of lithology and age

Tml **Lower, calcareous unit (middle and early Miocene)**—Calcareous, siliceous, and phosphatic, white- to tan-weathering mudstone and shale, with subordinate amounts of dolomite, porcelanite, breccia, glauconitic sandstone, and tuff. In places, unit exhibits intraformational deformation (including breccia) that may have formed by gravitational slumping shortly after deposition

Tr **Rincon Shale (early Miocene)**—Marine, primarily massive and thick-bedded, light-brown-weathering mudstone, with subordinate amounts of dolomite, siliceous shale, sandstone, and tuff. Mudstone is bioturbated, massive, and hackly fractured; locally, contains abundant microfossils. Single or multiple white-weathering tuff layers limited to upper 10 m of unit

Tv **Vaqueros Formation (early Miocene)**—Shallow-marine, massive and bioturbated, resistant, light-tan-weathering sandstone. Uppermost part consists of thinly interbedded sandstone, siltstone, and mudstone; base typically is marked by 50- to 150-cm-thick, thinly bedded, calcareous conglomerate containing abundant fossil-shell fragments

Sespe Formation (early Miocene to late Eocene)

Tspu **Upper unit (early Miocene and late Oligocene)**—Interbedded, thin- to thick-bedded sandstone, siltstone, and mudstone; weathers to various shades of maroon, buff, pale green, tan, and gray; proportions of different sedimentary rock types vary both laterally and vertically throughout section

Tspm **Middle unit (Oligocene)**—Interbedded conglomerate, sandstone, and mudstone; weathers to various shades of maroon, tan, and pale-greenish gray; proportions of different sedimentary rock types vary both laterally and vertically throughout section. Polymict conglomerates contain abundant chert and lithic sandstone clasts

Tspl **Lower unit (early Oligocene and late Eocene)**—Interbedded conglomerate, conglomeratic sandstone, sandstone, mudstone, and minor amounts of shale; weathers to various distinctive shades of salmon gray, reddish gray, pale-pinkish gray, and tan; proportions of different sedimentary rock types vary both laterally and vertically throughout section. Sandstones commonly are arkosic, and conglomerates contain rounded quartzitic, granitoid, metamorphic, and volcanic clasts

Tcw **Coldwater Sandstone (late? and middle Eocene)**—Shallow-marine, thin- to thick-bedded sandstone, which weathers to distinctive pale shades of buff, yellow, tan, and brown, and subordinate amounts of interbeds and thin intervals of gray, olive-gray, and

greenish-gray siltstone, shale, and mudstone; sandstone beds are resistant and form hogbacks where steeply dipping; upper part of unit locally is conglomeratic and rich in fossil oyster shells

Tcw-sh **Shale unit (late? and middle Eocene)**—Greenish-gray siltstone, with occasional interbeds of tan sandstone

Acknowledgments

This publication was funded by the California Ocean Protection Council and the U.S. Geological Survey (USGS) Coastal and Marine Geology Program. We are very grateful to USGS editor Taryn Lindquist for helping us develop the templates and formats for this series of publications, and for invaluable editorial review and suggestions. Patrick Barnard and Ann Gibbs (both USGS) provided constructive technical reviews.

References Cited

Anderson, T.J., Cochrane, G.R., Roberts, D.A., Chezar, H., and Hatcher, G., 2007, A rapid method to characterize seabed habitats and associated macro-organisms, *in* Todd, B.J., and Greene, H.G., eds., Mapping the seafloor for habitat characterization: Geological Association of Canada Special Paper 47, p. 71–79.

Barnard, P.L., Revell, D.L., Hoover, D., Warrick, J., Brocatus, J., Draut, A.E., Dartnell, P., Elias, E., Mustain, N., Hart, P.E., and Ryan, H.F., 2009, Coastal processes study of Santa Barbara and Ventura Counties, California: U.S. Geological Survey Open-File Report 2009–1029, 926 p., available at http://pubs.usgs.gov/of/2009/1029/.

Barnum, H.P., 1998, Redevelopment of the western portion of the Rincon offshore oil field, Ventura, California, *in* Kunitomi, D.S., Hopps, T.E., and Galloway, J.M., eds., Structure and petroleum geology, Santa Barbara Channel, California: American Association of Petroleum Geologists, Pacific Section, and Coast Geological Society, Miscellaneous Publication 46, p. 201–215.

Bascom, W., Mearns, A.J., and Moore, M.D., 1976, A biological survey of oil platforms in the Santa Barbara Channel: Journal of Petroleum Technology, v. 28, no. 1, p. 1,280–1,284.

Briggs, J.C., 1974, Marine zoogeography: New York, McGraw-Hill, 480 p.

Caldwell, R.J., Taylor, L.A., Eakins, B.W., Carignan, K.S., Grothe, P.R., Lim, E., and Friday, D.Z., 2010, Digital elevation models of Santa Monica, California—Procedures, data sources, and analysis: NOAA Technical Memorandum NESDIS NGDC-46, NOAA National Geophysical Data Center, available at http://www.ngdc.noaa.gov/dem/squareCellGrid/download/663.

California Department of Fish and Game, 2008, California Marine Life Protection Act master plan for marine protected areas—Revised draft: California Department of Fish and Game, accessed April 5, 2011, at http://www.dfg.ca.gov/mlpa/masterplan.asp.

Carignan, K.S., Taylor, L.A., Eakins, B.W., Warnken, R.R., Lim, E., and Medley, P.R., 2009, Digital elevation model of Santa Barbara, California—Procedures, data sources, and analysis: NOAA Technical Memorandum NESDIS NGDC-29, NOAA National Geophysical Data Center, available at http://www.ngdc.noaa.gov/dem/squareCellGrid/download/603.

Clarke, K.C., and Hemphill, J.J., 2002, The Santa Barbara oil spill—A retrospective, *in* Danta, D., ed., Yearbook of the Association of Pacific Coast Geographers: Honolulu, University of Hawai'i Press, v. 64, p. 157–162.

Cochrane, G.R., 2008, Video-supervised classification of sonar data for mapping seafloor habitat, *in* Reynolds, J.R., and Greene, H.G., eds., Marine habitat mapping technology for Alaska: Fairbanks, University of Alaska, Alaska Sea Grant College Program, p. 185–194, accessed February 20, 2013, at http://doc.nprb.org/web/research/research%20pubs/615_habitat_mapping_workshop/Individual%20Chapters%20High-Res/Ch13%20Cochrane.pdf.

Cochrane, G.R., Conrad, J.E., Reid, J.A., Fangman, S., and Golden, N., 2005, Nearshore benthic habitat GIS for the Channel Islands National Marine Sanctuary and southern California state fisheries reserves, volume II: U.S. Geological Survey Open-File Report 2005–1170, accessed February 20, 2013, at http://pubs.usgs.gov/of/2005/1170/.

Cochrane, G.R., and Lafferty, K.D., 2002, Use of acoustic classification of sidescan sonar data for mapping benthic habitat in the Northern Channel Islands, California: Continental Shelf Research, v. 22, p. 683–690.

Cochrane, G.R., Golden, N.E., Dartnell, P., Schroeder, D.M., and Finlayson, D.P., 2007, Seafloor mapping and benthic habitat GIS for southern California, volume III: U.S. Geological Survey Open-File Report 2007–1271, available at http://pubs.usgs.gov/of/2007/1271/.

Cochrane, G.R., Nasby, N.M., Reid, J.A., Waltenberger, B., and Lee, K.M., 2003, Nearshore benthic habitat GIS for the Channel Islands National Marine Sanctuary and southern California state fisheries

reserves, volume 1: U.S. Geological Survey Open-File Report 03–85, accessed February 20, 2013 at http://geopubs.wr.usgs.gov/open-file/of03-85/.
Dahlen, M.Z., 1992, Sequence stratigraphy, depositional history, and middle to late Quaternary sea levels of the Ventura shelf, California: Quaternary Research, v. 38, p. 234–245.
Dibblee, T.W., Jr., 1986, Geologic map of the Carpinteria quadrangle, Santa Barbara County, California: Santa Barbara, Calif., Dibblee Geological Foundation Map DF–04, scale 1:24,000.
Donnellan, A., Hager, B.H., and King, R.W., 1993, Discrepancy between geologic and geodetic deformation rates in the Ventura basin: Nature, v. 346, p. 333–336.
Drake, D.E., 1972, Distribution and transport of suspended matter, Santa Barbara Channel, California: Los Angeles, University of Southern California, Ph.D. dissertation, 358 p.
Draut, A.E., Hart, P.E., Lorenson, T.D., Ryan, H.F., Wong, F.L., Sliter, R.W., and Conrad, J.E., 2009, Late Pleistocene to Holocene sedimentation and hydrocarbon seeps on the continental shelf of a steep, tectonically active margin, southern California, USA: Marine Geophysical Research, v. 30, p. 193–206, doi:10.1007/s11001-009-9076-y.
Fader, G.B.J., 1997, Effects of shallow gas on seismic-reflection profiles, *in* Davies, T.A., Bell, T., Cooper, A.K., Josenhaus, H., Polyak, L., Solheim, A., Stoker, M.S., and Stravers, J.A., eds., Glaciated continental margins—An atlas of acoustic images: London, Chapman & Hall, p. 29–30.
Fairbanks, R.G., 1989, A 17,000-year glacio-eustatic sea level record—Influence of glacial melting rates on the Younger Dryas event and deep-ocean circulation: Science, v. 342, p. 637–642.
Fisher, M.A., Sorlien, C.C., and Sliter, R.W., 2009, Potential earthquake faults offshore southern California from the eastern Santa Barbara channel to Dana Point, *in* Lee, H.J., and Normark, W.R., eds., Earth science in the urban ocean—The Southern California Continental Borderland: Geological Society of America Special Paper 454, p. 271–290.
Fleming, K., Johnston, P., Zwartz, D., Yokoyama, Y., Lambeck, K., and Chappell, J., 1998, Refining the eustatic sea-level curve since the Last Glacial Maximum using far- and intermediate-field sites: Earth and Planetary Science Letters, v. 163, p. 327–342, doi:10.1016/S0012-821X(98)00198-8.
Galloway, J.M., 1997, Santa Barbara-Ventura basin province, *in* Dunkel, C.A., and Piper, K.A. eds., 1995 National assessment of United States oil and gas resources assessment of the Pacific outer continental shelf region: Minerals Management Service, Pacific OCS Region, Office of Resource Evaluation, OCS Report MMS 92–0019, p. 96–115.
Galloway, J.M., 1998, Chronology of petroleum exploration and development in the Santa Barbara channel area, offshore southern California, *in* Kunitomi, D.S., Hopps, T.E., and Galloway, J.M., eds., Structure and petroleum geology, Santa Barbara Channel, California: American Association of Petroleum Geologists, Pacific Section, and Coast Geological Society, Miscellaneous Publication 46, p. 1–12, 1 sheet.
Greene, H.G., Bizzarro, J.J., O'Connell, V.M., and Brylinsky, C.K., 2007, Construction of digital potential marine benthic habitat maps using a coded classification scheme and its application, *in* Todd, B.J., and Greene, H.G., eds., Mapping the seafloor for habitat characterization: Geological Association of Canada Special Paper 47, p. 141–155.
Greene, H.G., Bizzarro, J.J., Tilden, J.E., Lopez, H.L., and Erdey, M.D., 2005, The benefits and pitfalls of geographic information systems in marine benthic habitat mapping, *in* Wright, D.J., and Scholz, A.J., eds., Place matters: Portland, Oregon State University Press, p. 34–46.
Greene, H.G., Yoklavich, M.M., Starr, R.M., O'Connell, V.M., Wakefield, W.W., Sullivan, D.E., McRea, J.E., and Caillet, G.M., 1999, A classification scheme for deep seafloor habitats: Oceanologica Acta, v. 22, p. 663–678.
Griggs, G., Patsch, K., and Savoy, L., 2005, Living with the changing California coast: Berkeley, University of California Press, 540 p.

Gutierrez, C.I., Tan, S.S., and Clahan, K.B., 2008, Geologic map of the east half Santa Barbara 30′ × 60′ quadrangle, California: California Geological Survey, scale 1:100,000, available at ftp://ftp.consrv.ca.gov/pub/dmg/rgmp/Prelim_geo_pdf/SantaBarbara100keast.pdf.

Hapke, C.J., Reid, D., Richmond, B.B., Ruggiero, P., and List, J., 2006, National assessment of shoreline change part 3—Historical shoreline change and associated coastal land loss along sandy shorelines of the California Coast; U.S. Geological Survey Open-File Report 2006–1219, 72 p., accessed February 20, 2013, at http://pubs.usgs.gov/of/2006/1219/.

Heck, R.G., 1998, Santa Barbara Channel regional formline map, top Monterey Formation, *in* Kunitomi, D.S., Hopps, T.E., and Galloway, J.M., Structure and petroleum geology, Santa Barbara Channel, California: American Association of Petroleum Geologists, Pacific Section, and Coast Geological Society, Miscellaneous Publication 46, 1 plate.

Hornafius, J.S., Luyendyk, B.P., Terres, R.R., and Kamerling, M.J., 1986, Timing and extent of Neogene rotation in the western Transverse Ranges, California: Geological Society of America Bulletin, v. 97, p. 1,476–1,487.

Hovland, M., and Judd, A.G., 1988, Seabed pockmark and seepages: London, Graham and Trotman, Inc., 293 p.

Jackson, P.A., and Yeats, R.S., 1982, Structural evolution of Carpinteria basin, western Transverse Ranges, California: American Association of Petroleum Geologists Bulletin, v. 66, p. 805–829.

Jennings, C.W., and Bryant, W.A., 2010, Fault activity map of California: California Geological Survey Geologic Data Map no. 6, scale 1:750,000.

Johnson, S.Y., Sliter, R.W., Ritchie, A.C., Draut, A.E., and Hart, P.E., 2013, Seismic-reflection profiles, Offshore of Ventura map area, California, *sheet 8 in* Johnson, S.Y., Dartnell, P., Cochrane, G.R., Golden, N.E., Phillips, E.L., Ritchie, A.C., Kvitek, R.G., Greene, H.G., Krigsman, L.M., Endris, C.A., Seitz, G.G., Gutierrez, C.I., Sliter, R.W., Erdey, M.D., Wong, F.L., Yoklavich, M.M., Draut, A.E., and Hart, P.E. (S.Y. Johnson and S.A. Cochran, eds.), California State Waters Map Series—Offshore of Ventura, California: U.S. Geological Survey Scientific Investigations Map 3254, pamphlet 42 p., 11 sheets, scale 1:24,000, available at http://pubs.usgs.gov/sim/3254/.

Keller, E.A., and Gurrola, L.D., 2000, Final report, July, 2000—Earthquake hazard of the Santa Barbara fold belt, California: NEHRP Award #99HQGR0081, SCEC Award #572726, 78 p., last accessed April, 2011, at http://www.scec.org/research/98research/98gurrolakeller.pdf.

Kern, J.P., 1977, Origin and history of upper Pleistocene marine terraces, San Diego, California: Geological Society of America Bulletin, v. 88, p. 1,553–1,566.

Kvitek, R., 2007, California State University, Monterey Bay, Seafloor Mapping Lab Data Library: California State University, Monterey Bay, Seafloor Mapping Lab database, accessed May 12, 2011, at http://seafloor.csumb.edu/SFMLwebDATA.htm.

Kvitek, R., Bretz, C., Cochrane, G., and Greene, H.G., 2006, Statewide Marine Mapping Planning Workshop Final Report, December 12–13, 2005, Seaside, Calif.: California State University, Monterey Bay, 108 p., accessed February 20, 2013, at http://euclase.csumb.edu/DATA_DOWNLOAD/StrategicMapgWrkshp05/MappingWorkshop12_12-13/Final_Report/CA%20Habitat%20Mapping%20Rpt.pdf.

Kvitek, R.G., Phillips, E.L., and Dartnell, P., 2012, Colored shaded-relief bathymetry, Hueneme Canyon and vicinity, California, *sheet 1 in* Johnson, S.Y., Dartnell, P., Cochrane, G.R., Golden, N.E., Phillips, E.L., Ritchie, A.C., Kvitek, R.G., Greene, H.G., Krigsman, L.M., Endris, C.A., Clahan, K.B., Sliter, R.W., Wong, F.L., Yoklavich, M.M., and Normark, W.R. (S.Y. Johnson, ed.), California State Waters Map Series—Hueneme Canyon and vicinity, California: U.S. Geological Survey Scientific Investigations Map 3225, pamphlet 41 p., 12 sheets, available at http://pubs.usgs.gov/sim/3225/.

Lajoie, K.R., Ponti, D.J., Powell, C.L., II, Mathieson, S.A., and Sarna-Wojcicki, A.M., 1991, Emergent marine strandlines and associated sediments, coastal California—A record of Quaternary sea-level fluctuations, vertical tectonic movements, climatic changes, and coastal processes, *in* Morrison, R.B.,

ed., The Geology of North America, Quaternary nonglacial geology, Conterminous U.S.: Geological Society of America Decade of North American Geology, v. K-2, p. 190–214.
Lajoie, K.R., Sarna-Wojcicki, A.M., and Yerkes, R.F., 1982, Quaternary chronology and rates of crustal deformation in the Ventura area, California, *in* Cooper, J.D., comp., Neotectonics in southern California: April 1982, 78th Annual Meeting, Geological Society of America Cordilleran Section, Guidebook, Field Trip 3, p. 43–52.
Lambeck, K., and Chappell, J., 2001, Sea level change through the last glacial cycle: Science, v. 292, p. 679–686, doi:10.1126/science.1059549.
Larson, K.M., and Webb, F.H., 1992, Deformation in the Santa Barbara Channel from GPS measurements 1987–1991: Geophysical News Letters, v. 19, p. 1,491–1,494.
Lee, H.J., and Normark, W.R., eds., 2009, Earth science in the urban ocean—The Southern California Continental Borderland: Geological Society of America Special Paper 454, 481 p.
Lee, W.H.K., and Vedder, J.G., 1973, Recent earthquake activity in the Santa Barbara Channel region: Bulletin of the Seismological Society of America, v. 63, p. 1,757–1,773.
Luyendyk, B.P., Kamerling, M.J., and Terres, R.R., 1980, Geometric model for Neogene crustal rotations in southern California: Geological Society of America Bulletin, v. 91, p. 211–217.
Madden, C.J., Goodin, K.L., Allee, R., Finkbeiner, M., and Bamford, D.E., 2008, Draft Coastal and Marine Ecological Classification Standard: National Oceanic and Atmospheric Administration (NOAA) and NatureServe, v. III, 77 p.
Minor, S.A., Kellogg, K.S., Stanley, R.G., Gurrola, L.D., Keller, E.A., and Brandt, T.R., 2009, Geologic map of the Santa Barbara coastal plain area, Santa Barbara County, California: U.S. Geological Survey Scientific Investigations Map 3001, scale 1:25,000, 1 sheet, pamphlet 38 p., available at http://pubs.usgs.gov/sim/3001/.
Mitchum, R.M., Jr., Vail, P.R., and Sangree, J.B., 1977, Seismic stratigraphy and global changes of sea level, part 6—Stratigraphic interpretation of seismic reflection patterns in depositional sequences, *in* Payton, C.E., ed., Seismic stratigraphy—Applications to hydrocarbon exploration: Tulsa, Okla., American Association of Petroleum Geologists, p. 117–133.
National Oceanic and Atmospheric Administration, 2011, Coastal ifSAR: Digital Coast, NOAA Coastal Services Center database, accessed April 5, 2011, at http://www.csc.noaa.gov/digitalcoast/.
Nicholson, C., Sorlien, C., Atwater, T., Crowell, J.C., and Luyendyk, B.P., 1994, Microplate capture, rotation of the western Transverse Ranges, and initiation of the San Andreas transform as a low-angle fault system: Geology, v. 22, p. 491–495.
Nicholson, C., Kamerling, M.J., and Sorlien, C.C., 2005, Kinematic mapping of 3D fault planes in southern California: U.S. Geological Survey Final Technical Report, Award No. 03HQGR0021, 16 p., accessed April 5, 2011, at http://earthquake.usgs.gov/research/external/reports/03HQGR0021.pdf.
Normark, W.R., Piper, D.J.W., Romans, B.W., Covault, J.A., Dartnell, P., and Sliter, R.W., 2009, Submarine canyon and fan systems of the California Continental Borderland, *in* Lee, H.J., and Normark, W.R., eds., Earth science in the urban ocean—The Southern California Continental Borderland: Geological Society of America Special Paper 454, p. 141–168.
O'Reilly, W.C., and Guza, R.T., 1993, A comparison of spectral wave models in the Southern California Bight: Coastal Engineering, v. 19, p. 263–282, doi:10.1016/0378-3839(93)90032-4.
Peltier, W.R., 2005, On the hemispheric origins of meltwater pulse 1a: Quaternary Science Reviews, v. 24, p. 1,655-1,671.
Peltier, W.R., and Fairbanks, R.G., 2006, Global glacial ice volume and Last Glacial Maximum duration from an extended Barbados sea level record: Quaternary Science Reviews, v. 25, p. 3,322–3,337.
Petersen, M.D., Frankel, A.D., Harmsen, S.C., Mueller, C.S., Haller, K.M., Wheeler, R.L., Wesson, R.L., Zeng, Y., Boyd, O.S., Perkins, D.M., Luco, N., Field, E.H., Wills, C.J., and Rukstales, K.S., 2008, Documentation for the 2008 update of the United States National Seismic Hazard Maps: U.S.

Geological Survey Open-File Report 2008–1128, 61 p., accessed April 5, 2011, at http://pubs.usgs.gov/of/2008/1128/.
Redin, T., Forman, J., and Kamerling, M.J., 1998, Regional structure section across the eastern Santa Barbara Channel, from eastern Santa Cruz Island to the Carpinteria area, Santa Ynez Mountains, *in* Kunitomi, D.S., Hopps, T.E., and Galloway, J.M., eds., Structure and petroleum geology, Santa Barbara Channel, California: American Association of Petroleum Geologists, Pacific Section, and Coast Geological Society, Miscellaneous Publication 46, p. 195–200, 1 sheet.
Redin, T., Kamerling, M.J., and Forman, J., 2004, Santa Barbara Channel structure and correlation sections—Correlation section no. 34R., N–S structure and correlation section, south side central Santa Ynez Mountains across the Santa Barbara channel to the east end of Santa Cruz Island: American Association of Petroleum Geologists, Pacific Section, Publication CS 32, 1 sheet.
Reid, J.A., Reid, J.M., Jenkins, C.J., Zimmerman, M., Williams, S.J., and Field, M.E., 2006, usSEABED—Pacific Coast (California, Oregon, Washington) offshore surficial-sediment data release: U.S. Geological Survey Data Series 182, available at http://pubs.usgs.gov/ds/2006/182/.
Rockwell, T.K., Keller, E.A., and Dembroff, G.R., 1988, Quaternary rate of folding of the Ventura Avenue anticline, western Transverse Ranges, southern California: Geological Society of America Bulletin, v. 100, p. 850–858.
Slater, R.A., Gorsline, D.S., Kolpack, R.L., and Shiller, G.I., 2002, Post-glacial sediments of the California shelf from Cape San Martin to the US-Mexico border: Quaternary International, v. 92, p. 45–61.
Sliter, R.W., Triezenberg, P.J., Hart, P.E., Draut, A.E., Normark, W.R., and Conrad, J.E., 2008, High-resolution chirp and mini-sparker seismic-reflection data from the southern California continental shelf—Gaviota to Mugu Canyon: U.S. Geological Survey Open-File Report 2008–1246, accessed April 5, 2011, at http://pubs.usgs.gov/of/2008/1246/.
Sommerfield, C.R., Lee, H.J., and Normark, W.R., 2009, Postglacial sedimentary record of the southern California continental shelf and slope, Point Conception to Dana Point, *in* Lee, H.J., and Normark, W.R., eds., Earth science in the urban ocean—The Southern California Continental Borderland: Geological Society of America Special Paper 454, p. 89–116.
Sorlien, C.C., Gratier, J.P., Luyendyk, B.P., Hornafius, J.S., and Hopps, T.E., 2000, Map restoration of folded and faulted late Cenozoic strata across the Oak Ridge fault, onshore and offshore Ventura basin, California: Geological Society of America Bulletin, v. 112, p. 1,080–1,090.
Southern California Earthquake Data Center, 2010, Southern California Earthquake Catalog: Southern California Earthquake Data Center database, accessed April 5, 2011, at http://www.data.scec.org/eqcatalogs/index.html.
Stanford, J.D., Hemingway, R., Rohling, E.J., Challenor, P.G., Medina-Elizalde, M., and Lester, A.J., 2011, Sea-level probability for the last deglaciation—A statistical analysis of far-field records: Global and Planetary Change, v. 79, p. 193–203.
Sylvester, A.G., 2001, Catalog of Santa Barbara earthquakes—1800 to 1960: University of California, Santa Barbara, database, accessed April 5, 2011, at http://projects.crustal.ucsb.edu/sb_eqs/SBEQCatlog/SBEQCATINTRO.html, last accessed April, 2011.
Sylvester, A.G., Smith, S.S., and Scholz, C.H., 1970, Earthquake swarm in the Santa Barbara Channel, California, 1968: Bulletin of the Seismological Society of America, v. 60, p. 1,047–1,060.
Tan, S.S., and Clahan, K.B., 2004, Geologic map of the White Ledge Peak 7.5′ quadrangle, Santa Barbara and Ventura Counties, California—A digital database: California Geological Survey Preliminary Geologic Map, scale 1:24,000, available at http://www.conservation.ca.gov/cgs/rghm/rgm/preliminary_geologic_maps.htm.
Tan, S.S., Jones, T.A., and Clahan, K.B., 2003a, Geologic map of the Pitas Point 7.5′ quadrangle, Ventura County, California—A digital database: California Geological Survey Preliminary Geologic

Map, scale 1:24,000, available at http://www.conservation.ca.gov/cgs/rghm/rgm/preliminary_geologic_maps.htm.
Tan, S.S., Jones, T.A., and Clahan, K.B., 2003b, Geologic map of the Ventura 7.5′ quadrangle, Ventura County, California—A digital database: California Geological Survey Preliminary Geologic Map, scale 1:24,000, available at http://www.conservation.ca.gov/cgs/rghm/rgm/preliminary_geologic_maps.htm.
Tissot, B.N., Yoklavich, M.M., Love, M.S., York, K., and Amend, M., 2006, Benthic invertebrates that form habitat on deep banks off southern California, with special reference to deep sea coral: Fishery Bulletin, v. 104, p. 167–181.
Trecker, M.A., Gurrola, L.D., and Keller, E.A., 1998, Oxygen-isotope correlation of marine terraces and uplift of the Mesa Hills, Santa Barbara, California, USA, *in* Stewart, I.S., and Vita-Finzi, C., eds., Coastal tectonics: Geological Society of London Special Publications, v. 146, p. 57–69.
U.S. Geological Survey, 2009, National Archive of Marine Seismic Surveys: U.S. Geological Survey database, accessed April 5, 2011, at http://walrus.wr.usgs.gov/NAMSS/.
Warrick, J.A., and Farnsworth, K.L., 2009, Sources of sediment to the coastal waters of the Southern California Bight, *in* Lee, H.J., and Normark, W.R., eds., Earth science in the urban ocean—The Southern California Continental Borderland: Geological Society of America Special Paper 454, p. 39–52.
Weber, K.M., List, J.H., and Morgan, K.L., 2005, An operational Mean High Water datum for determination of shoreline position from topographic lidar data: U.S. Geological Survey Open-File Report 2005–1027, accessed April 5, 2011, at http://pubs.usgs.gov/of/2005/1027/.
Wills, C.J., Weldon, R.J., II, and Bryant, W.A., 2008, Appendix A—California fault parameters for the National Seismic Hazard Maps and Working Group on California Earthquake Probabilities 2007: U.S. Geological Survey Open File Report 2007–1437A, 48 p., available at http://pubs.usgs.gov/of/2007/1437/a/.
Wong, F.L., Phillips, E.L., Johnson, S.Y, and Sliter, R.W., 2012, Modeling of depth to base of Last Glacial Maximum and seafloor sediment thickness for the California State Waters Map Series, eastern Santa Barbara Channel, California: U.S. Geological Survey Open-File Report 2012–1161, 16 p., available at http://pubs.usgs.gov/of/2012/1161/.
Xu, J.P., and Noble, M.A., 2009, Variability of the southern California wave climate and implications for sediment transport, *in* Lee, H.J., and Normark, W.R., eds., Earth science in the urban ocean—The Southern California Continental Borderland: Geological Society of America Special Paper 454, p. 171–192.